PROGRESS REPORT

ADVANCED MATERIALS
www.advmat.de

Photoprogrammable Mesogenic Soft Helical Architectures: A Promising Avenue toward Future Chiro-Optics

Zhi-Gang Zheng, Yan-Qing Lu,* and Quan Li**

Mesogenic soft materials, having single or multiple mesogen moieties per molecule, commonly exhibit typical self-organization characteristics, which promotes the formation of elegant helical superstructures or supramolecular assemblies in chiral environments. Such helical superstructures play key roles in the propagation of circularly polarized light and display optical properties with prominent handedness, that is, chiro-optical properties. The leveraging of light to program the chiro-optical properties of such mesogenic helical soft materials by homogeneously dispersing photosensitive chiral material into an achiral soft system or covalently connecting photochromic moieties to the molecules has attracted considerable attention in terms of materials, properties, and potential applications and has been a thriving topic in both fundamental science and application engineering. State-of-the-art technologies are described in terms of the material design, synthesis, properties, and modulation of photoprogrammable chiro-optical mesogenic soft helical architectures. Additionally, the scientific issues and technical problems that hinder further development of these materials for use in various fields are outlined and discussed. Such photoprogrammable mesogenic soft helical materials are competitive candidates for use in stimulus-controllable chiro-optical devices with high optical efficiency, stable optical properties, and easy miniaturization, facilitating the future integration and systemization of chiro-optical chips in photonics, photochemistry, biomedical engineering, chemical engineering, and beyond.

1. Introduction

Chiral molecules, which are omnipresent in nature in biological organisms,[1] medicine, genes,[2] neurons,[3] and so on, feature non-superimposed mirror image molecular structures, resulting in a certain handedness determined by the corresponding enantiomer. The introduction of a stereocenter or axial chirality into a molecule produces a remarkable helical superstructure configuration due to the facility of molecular self-organization and the delicate interplay of intra- and intermolecular interactions. The gathering of several or hundreds of chiral molecules through non-covalent interactions, for example, hydrogen or halogen bonds, produces aggregates with distinct properties that single molecules cannot exhibit. In turn, these aggregates enable the formation of advanced supramolecular assemblies (**Figure 1**A),[4] which generally exist in polymers and some oligomers. On the other hand, molecular rearrangement driven by a phase transition forms certain spatial structures with molecules regularly located at equilibrium positions, referred to as superstructure, such as the typical liquid crystalline 1D periodic cholesteric phase (Figure 1B-a) and chiral cubic blue phase (BP) (Figure 1B-b).[5]

This elegant helical superstructure establishes a bridge between the molecular and wavelength scales and is generally accompanied by a specific optical activity, that is, the polarization of linearly polarized light rotates according to the handedness of the chiral medium. This activity is mainly attributable to the difference between the optical refractive indices of right- and left-handed circularly polarized light (CPL), resulting in unique and prominent chiral dependency of the propagation, transmission, reflection, and absorption, that is, chiro-optical characteristics. Two representative chiro-optical effects that are often of interest are selective photonic bandgaps (PBGs) and circular dichroism (CD). In some optical anisotropic media such as liquid crystals (LCs) and other self-assembled mesoscale materials, the helical superstructure enables periodic refractive index modulation in the direction of the helical axis according to the polarization of the incident light. Such periodic modulation, which closely resembles the behavior of a photonic crystal complying with the Bragg reflection law, that is, selective

Prof. Z.-G. Zheng
Department of Physics
East China University of Science and Technology
Shanghai 200237, China
E-mail: zgzheng@ecust.edu.cn

Prof. Y.-Q. Lu
National Laboratory of Solid State Microstructures
Key Laboratory of Intelligent Optical Sensing and Manipulation
Collaborative Innovation Center of Advanced Microstructures
and College of Engineering and Applied Sciences
Nanjing University
Nanjing 210093, China
E-mail: yqlu@nju.edu.cn

Prof. Q. Li
Advanced Materials and Liquid Crystal Institute and Chemical Physics Interdisciplinary Program
Kent State University
Kent, OH 44242, USA
E-mail: qli1@kent.edu

The ORCID identification number(s) for the author(s) of this article can be found under https://doi.org/10.1002/adma.201905318.

DOI: 10.1002/adma.201905318

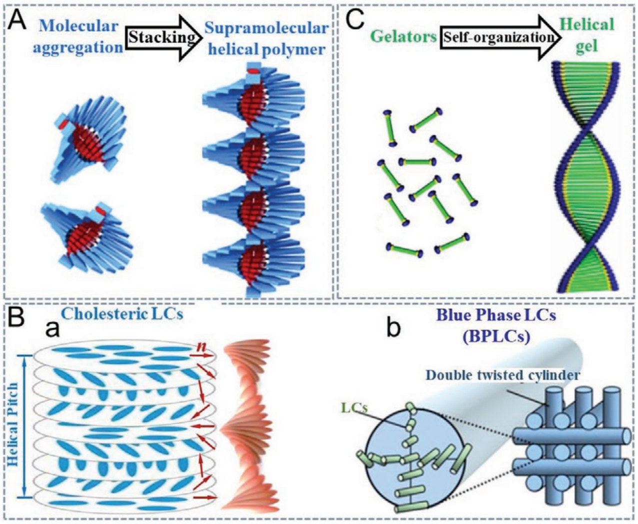

Figure 1. Self-organized helical mesogenic soft materials. A) Helical polymer formed by the stacking of molecular aggregates. B) Self-organized LC helical superstructure showing: a) a 1D helix (i.e., the cholesteric phase) and b) a 3D cubic structure (i.e., the BP). The red arrows in (a) denote the directions of the LC molecules; the cubic structure of the BP consists of stacked LC double-twisted cylinders. C) Illustration of self-organized helical gel. A) Reproduced with permission.[4a] Copyright 2012, Springer Nature. B) Reproduced with permission. [5a] Copyright 2008, Springer-Verlag GmbH.

reflection, exhibits photonic localization in the band gap determined by the period in the case of normal incidence.[6] Similarly, a helical superstructure composed of chiral chromophores leads to absorption differences between left- and right-handed CPL, referred to as the Cotton effect, owing to the asymmetry of chiral chromophores or that of achiral chromophores induced by a chiral system.[7]

Chiro-optical characteristics in helical supramolecular assemblies and superstructures have attracted tremendous attention in the past decade, especially in self-organized mesogenic helical soft matter, which is an emerging scientific frontier in chemistry, functional materials, soft matter physics, biological medicine, and even sensor physics. Mesogenic soft matter, defined as soft condensed matter with molecules containing single or multiple anisotropic mesogen moieties, is distinct from common soft condensed matter in terms of molecular arrangement, interaction, and specific optical chirality, although the "soft" characteristic is still maintained. A primary reason for the softness is related to the responses of this type of matter to multiple external stimuli, such as electric fields, heat, light, mechanical forces, and even acoustic fields.[8] The control and manipulation of such soft materials by light is always more desirable than that of other stimuli due to the prominent advantages of non-contact, wireless, remote, and high-resolution control, which enable numerous unprecedented chiro-optical applications.[9] Optically, another fascinating feature of these materials is their molecular self-organization behavior, which can establish an ordered and regular arrangement with a structural parameter (≈µm) much larger than the single-molecule scale (≈nm) through the weak non-covalent molecular interaction, rather than the chemical bonds that normally exist in

Zhi-Gang Zheng is a professor at the Department of Physics, East China University of Science and Technology (ECUST). He received his Ph.D. in optics and optical materials from Changchun Institute of Optics, Fine Mechanics and Physics, Chinese Academy of Sciences, in 2009. He then worked at Nanjing University and the Advanced Materials and Liquid Crystal Institute of Kent State University as a postdoctoral fellow, cooperating with Prof. Yan-Qing Lu and Prof. Quan Li, respectively. His research interest span from stimuli-responsive smart soft materials and advanced adaptive photonic materials to stimuli-controllable photonic devices and systems.

Yan-Qing Lu received his B.S. and Ph.D. degrees from Nanjing University, China, in 1991 and 1996, respectively. He has 5 years of experience in the U.S. and China telecomm industries. He designed and developed a serial of liquid-crystal-based fiber-optic devices with his colleagues, which include variable optical attenuators, variable Mux/Demux, and DWDM wavelength blockers. He is currently a Changjiang Distinguished Professor at Nanjing University. His research interests include liquid crystal photonics, fiber optics, and nonlinear optics.

Quan Li is Director of Organic Synthesis and Advanced Materials Laboratory at the Advanced Materials and Liquid Crystal Institute of Kent State University, where he is also Adjunct Professor in the Chemical Physics Interdisciplinary Program. He received his Ph.D. in organic chemistry from the Chinese Academy of Sciences in Shanghai, where he was promoted to Full Professor of organic chemistry and medicinal chemistry in February 1998. His current research interest spans from stimuli-responsive smart soft matter, advanced photonic and optoelectronic materials for energy-harvesting and energy-saving, and functional biocompatible materials and nanoparticles to nanoengineering and device fabrication.

solids.[10] Judicious molecular design together with precise control of the self-organization conditions facilitates the formation of well-defined soft helical superstructures possessing both optical chirality and photoresponsiveness, readily enabling the photoprogramming of chiro-optical characteristics, which breaks new ground for chiral soft matter toward both fundamental science and practical applications.

The chiro-optical phenomenon in mesogenic soft matter was observed almost 150 years ago (mainly focused on LCs), followed by gradual development that accelerated in the past decade. Contemporarily, ingenious photoresponsive chiro-optical soft materials with anisotropic mesogen moieties, including LCs, polymers, and gels (Figure 1C), have been proposed, designed, and prepared. Their typical chiro-optical effects, such as handedness-dependent reflection, absorption, and propagation of incident light, have also been explored thoroughly. Furthermore, light manipulation, optical chirality control and programming, and the corresponding applications were elaborately conceived and optimized.[11–13] However, no review or progress report exclusively concerning the chiro-optical characteristics, light manipulation, and perspective photonic applications of such soft materials is currently available. Hence, this report describes the state-of-the-art development of photoresponsive mesogenic helical soft materials. It provides robust demonstrations of two of the most representative chiro-optical properties, that is, handedness-dependent light propagation (the PBG effect) and absorption (CD), in the photoresponsive helical superstructures and supramolecular assemblies formed in LCs, polymers, and gels. Moreover, potential chiro-optical devices are discussed, including their design, manipulation, programmability, and performance. This review provides conceptual insight into chiro-optical mesogenic soft materials, which constitute a burgeoning interdisciplinary topic related to functional materials, soft condensed matter physics, optics, and organic chemistry, and creates an opportunity for scientists and engineers to recognize and reconsider this category of materials and structures. Section 2 demonstrates two types of typical photoresponsive chiro-optical mesogenic helical soft materials, featuring light-modulated PBGs and CD, and their applications. The summary and prospects are given in Section 3.

2. Photoresponsive Chiro-Optical Mesogenic Helical Soft Materials

2.1. Materials with Light-Modulated PBGs

A soft helical architecture organized by optically anisotropic units normally shows a conspicuous PBG effect with respect to certain CPL having the same handedness as the helix, that is, handedness-dependent PBG, which is entirely embodied in LCs, a typical type of optically anisotropic soft matter. During the past decades, the PBG effect was thoroughly investigated and developed, focusing on self-organized helical LCs. CPL with the same handedness as a helical LC material will be stopped provided that its wavelength falls within the PBG. The PBG, determined by the helical pitch length P, the average refractive index of the helical LCs $<n>$, and the incident angle θ, can be expressed as $\lambda_c = <n> P\cos\theta$, where λ_c is the central wavelength of the band. The bandwidth is $\Delta\lambda = \Delta n P\cos\theta$, where Δn is the birefringence of the LCs. In the case of normal incidence and for a given LC material, the central wavelength and bandwidth of the PBG are determined solely by the helical pitch. Because of the multi-field responses of LCs, electric fields were first utilized to modulate the pitch length considering compatibility with other electronic devices. Unfortunately, such modulation seems less effective in helical LCs due to the competition between dielectric and elastic torque. Therefore, establishing a more efficient means of generating reversible PBG modulation in a relatively wide spectral range is of high priority.

2.1.1. Helical LCs Containing Azobenzene-Based Chiral Materials

Azobenzene-based materials, which have photosensitive azo moieties embedded between pairs of phenyl groups, produce large molecular geometric deformation via the transformation between *trans*- and *cis*-isomers after light irradiation and thus are considered appropriate additives to endow common LCs with photoresponsive characteristics. Cholesteryl groups were decorated on either end of azobenzene molecules to produce a photosensitive chiral additive,[14] generating an interesting isothermal phase transition in the helical LC system that differed from the previously reported phase transition in nematic systems mixed with common rod-like azobenzenes.[15]

There have been persistent endeavors to enlarge the dynamic spectral range for the PBG further by replacing the chiral moiety from the original cholesteryl group with binaphthalene with an axial chirality to strengthen the helical twisting power (HTP) of the chiral dopant significantly in most LCs.[16–18] Two azo groups were judiciously decorated at the 2 and 2′ positions of binaphthalene to provide the material with in situ light-switchable HTP (**Figure 2**A-a I and II). Moreover, two mesogenic groups were properly connected on the opposite ends of the two azo groups to improve the compatibility of the chiral additive in LCs (Figure 2A-a III). Subsequent exploration revealed an HTP as high as 304 μm^{-1} in the initial state. The two photostationary states (PSSs) with corresponding HTPs of 89 and 198 μm^{-1} in the commercial E7 LCs exhibited impressive HTP modulation capabilities for such photoresponsive chiral dopants, resulting in a reversible shift of PBG covering the red, green, and blue bands without any change in helical handedness and enabling the fabrication of a light-driven colorful display prototype.[19–21] The subsequent structural modification of these chiral molecules on the terminal alkyl chain promoted completely distinct performance but maintained a sufficiently strong HTP, resulting in the production of three PSSs reflecting red, green, and blue when a sample was exposed to three different wavelengths (Figure 2A-b).[22] Furthermore, subtly bridging two binaphthalenes through an azo group furnished a photoresponsive chiral additive with both a large HTP and satisfactory light modulation.[23] However, the reversible modulation among red, green, and blue reflections can be implemented using visible light solely due to an extended conjugated molecular structure of the chiral dopant. Similarly, to extend the conjugation length, binaphthalene was decorated with two novel ortho-fluorinated azobenzene derivatives very recently, which not only produced a large HTP and excellent light modulation, but also a PBG that could be reversibly driven using 450 nm and 530 nm visible sources (Figure 2B).[24]

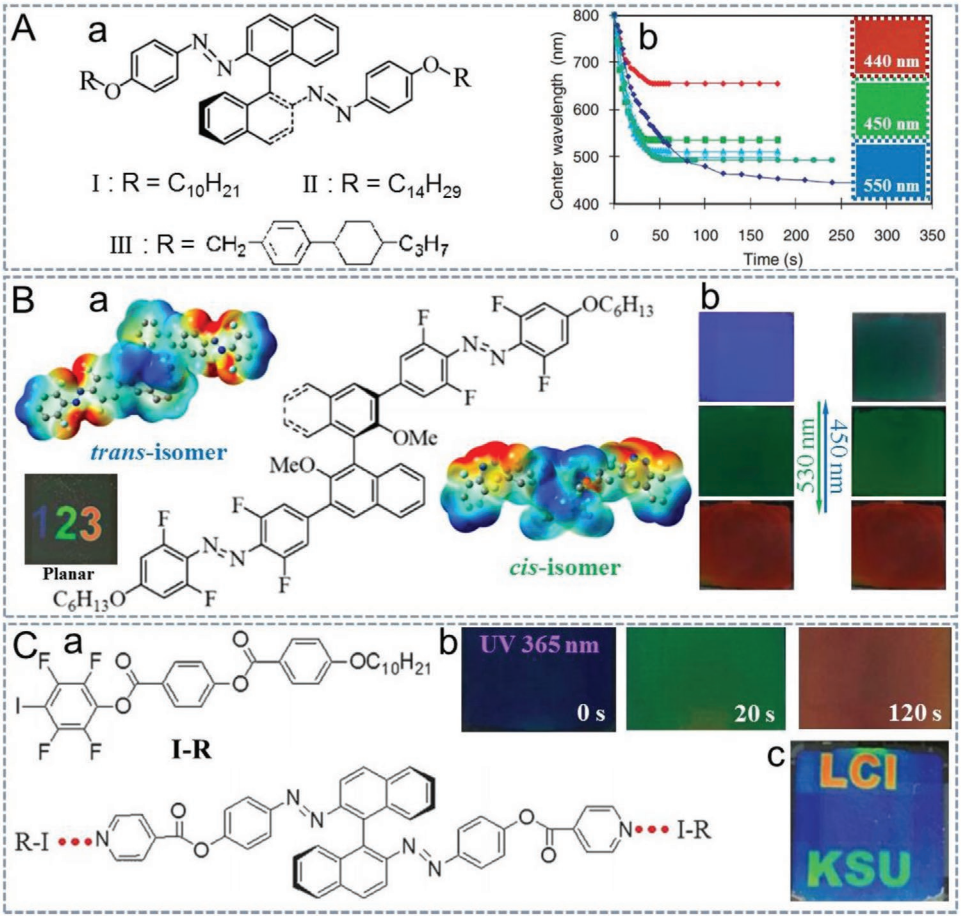

Figure 2. Light-modulated PBG of helical LCs enabled by photosensitive azobenzene-based binaphthalene chiral materials. A) PBG modulation based on commonly adopted chiral materials (a), where the stable PBGs reflected red, green, and blue light when the sample containing chiral material III (see (a)) was irradiated with three different wavelengths (b). B) Visible-light-modulated PBG enabled by fluorinated-azobenzene-decorated binaphthalene chiral material (a) and the corresponding reversible shift between the blue and red bands by irradiation with 530 nm and 450 nm visible light, respectively (b). The inset in the lower left corner of (b) depicts data photowriting in a planar LC cell. C) PBG modulation based on mesogenic halogen-bond donor I-R and an azobenzene-based binaphthalene chiral material as the halogen-bond acceptor mixed in an LC system (a), showing a shift from the blue band to the green band and subsequently to the red band upon 365 nm UV irradiation (b); c) the words "LCI" and "KSU" were written in a planar LC cell by UV exposure through the photomask. A-a-i,ii) Reproduced with permission.[19a] Copyright 2007, American Chemical Society. A-a-iii) Reproduced with permission.[21] Copyright 2010, The Royal Society of Chemistry. A-b) Reproduced with permission.[22] Copyright 2011, Wiley-VCH. B) Reproduced with permission.[24] Copyright 2019, American Chemical Society. C) Reproduced with permission.[25] Copyright 2018, Wiley-VCH.

The terminal group of the azobenzene-based binaphthalene axial chiral molecule was replaced with a halogen-bond acceptor, while a mesogenic achiral halogen-bond donor was mixed into the LCs to form a halogen bond with the chiral molecules and to enhance the molecular interaction between the chiral dopant and LCs (Figure 2C).[25] The PBG could be shifted from the original state reflecting a bluish color to a reddish PSS in a photoresponsive system containing a small amount of halogen-bonded chiral dopant (2.8 mol%) after irradiation with UV light for 2 min. It is worth mentioning here that similar wide spectral range modulation of PBG can be achieved by adjusting the temperature, which is probably related to the halogen-bond weakening upon heating.

2.1.2. Helical LCs Containing Diarylethene-Based Chiral Materials

Greater thermostability of chiral molecular switch is preferable for further chiro-optical applications, especially in situations involving digital control. One prominent issue with azobenzene-based chiral molecules is their thermal relaxation in the photoisomerized *cis* state. In other words, the *cis*-isomers should be transformed into the *trans*-conformation in the ground state, resulting in unstable chiral molecules in PSS states or other intermediate states. Therefore, it is advisable to design a molecular structure with improved thermostability. Dithienylcyclopentene-based chiro-optical molecules with two axial chiral centers provided by two bridged binaphthalene groups were synthesized previously (**Figure 3**A-a),[26] exhibiting excellent thermostability in the photoisomerization process due to the specific open- and closed-ring isomers generated via reversible cyclization. Moreover, HTPs higher than those of the previous materials were achieved, as well as an HTP change upon light irradiation.[27] The relatively high HTPs of this kind of chiral material in commercially available LCs (E7 or 5CB) in PSSs corresponding to 310 nm UV (i.e., $\mathrm{PSS_{UV}}$) and 550 nm visible light (i.e., $\mathrm{PSS_{Vis}}$) irradiation were more than 150 μm^{-1}

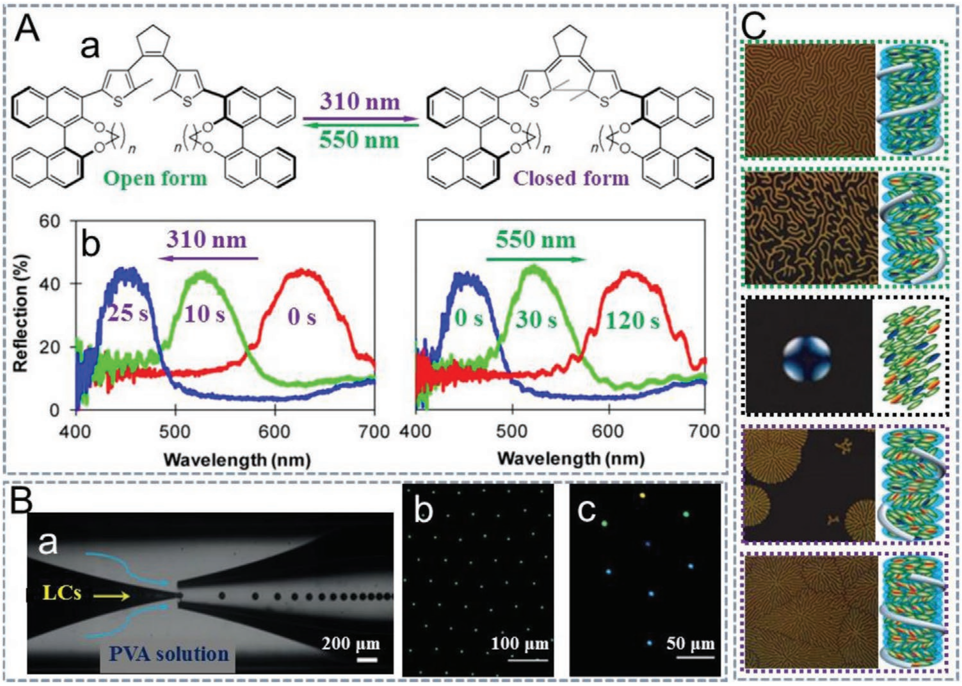

Figure 3. Helical superstructure modulations of both the PBG and handedness enabled by fatigue-resistant, diarylethene-based chiral materials. A) Several kinds of chiral materials with different lengths of the alkyl bridging two naphthalenes were designed (a), and chiral material with $n = 1$ was used for reversible light modulation of the PBG from the red to blue band (b). B) Chiral material with $n = 1$ was also adopted in the microdroplet generated by a capillary (a). The PBG modulation of the droplets is shown in (b) and (c) on different scales. C) Handedness inversion of the LC helix was achieved when the bridge length reached 4, that is, $n = 4$, presenting a gradual disappearance of the fingerprint optical texture, passing through an unwound dark state, and reoccurrence of a similar fingerprint texture with 310 nm light exposure. The right side of every sub-panel in (C) schematically shows the aforementioned process. A-a) Reproduced with permission.[29] Copyright 2013, Wiley-VCH. A-b) Reproduced with permission.[26a] Copyright 2012, American Chemical Society. B) Reproduced with permission.[28] Copyright 2015, Wiley-VCH. C) Reproduced with permission.[29] Copyright 2013, Wiley-VCH.

and 105 μm^{-1}, respectively, producing PBG modulation from the red to blue band by UV irradiation and recovery by visible light irradiation (Figure 3A-b).[26a] The molecular design of the dithienylcyclopentene-based chiral molecular switch, focusing on the substituents at the 6 and 6′ positions, indicates that properly connecting the rigid group can significantly increase the HTP values in both PSS$_{\mathrm{UV}}$ and PSS$_{\mathrm{Vis}}$, and the values are enhanced with lengthening of the rigid moiety since the interaction between the chiral molecules and LCs is stronger.[26c,d] As biphenyl was connected, the HTP exceeded 220 μm^{-1} in both PSSs, and considerable light modulation of the HTP remained, producing a similar PBG blue-shift from the red to blue band. Moreover, a chiro-optical micro-droplet of the LC helical superstructure was fabricated using a capillary-based microfluidic device (Figure 3B-a) to generate a light-modulated omnidirectional PBG effect (Figure 3B-b,c).[28]

However, different results were induced as the length of the alkylene bridge linking the 2 and 2′ positions of binaphthalene was varied (Figure 3A-a).[29] As the length of the alkylene bridge increased from one to three carbons, the HTP in PSS$_{\mathrm{UV}}$ gradually decreased, which may have been related to the weakening of the rotational restriction of the two naphthalene rings. Continuous extension to four carbons led to a remarkable handedness inversion from the initial right-handedness to left-handedness by UV irradiation, with recovery to right-handedness by changing from UV light to 550 nm visible light (Figure 3C). This handedness transformation of a helical superstructure via the photoisomerization of a molecular-scale chiral switch was probably caused by a larger geometric change of the chiral molecules from open- to closed-ring form due to the weak rotational restriction of two naphthalenes bridged by a longer alkylene linker.[30–32] A prominent advantage of such handedness-inversed chiral material is thermostability higher than that of azobenzene-based, handedness-inversed chiral material consisting of a binaphthalene moiety bonded to the meta-positions of azobenzene through two methylene chains.[33] The experimental results indicated that a right-handed LC helical superstructure, passing through an unwound nematic state, transformed to another helix with similar pitch length but opposite handedness, which reasonably manifested very distinct chiro-optical performance with modulations in both helical pitch and handedness, that is, the photonic band position and handedness of a CPL responding to the PBG effect can be dynamically controlled, operated, and programmed artificially.

2.1.3. Helical LCs Containing Rotary Chiral Molecular Motors

A photoresponsive chiral molecular motor based on biphenanthrylidene with two stereo-centers was proposed to achieve PBG modulation covering the entire visible spectral band.[34–36] The initial (*P*,*P*)-*trans* isomer transformed into an (*M*,*M*)-*cis* conformation upon irradiation by UV light with a wavelength longer than 280 nm; the (*M*,*M*)-*cis* isomer was converted into

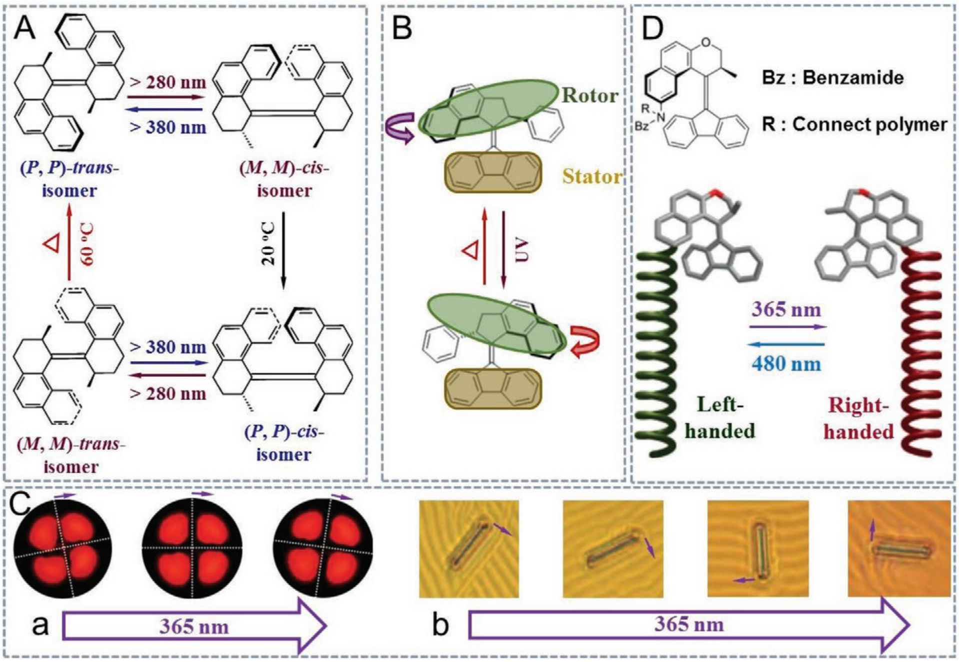

Figure 4. Helical pitch (i.e., PBG) modulation of LCs mixed with rotary chiral molecular motors. A) Isomerization of a molecule with two rotors that can be rotated around the C=C axis by UV irradiation. B) Second-generation chiral molecular motor with one stator and one rotor, that is, the rotor can be rotated anticlockwise by UV irradiation and clockwise upon thermal recovery. C) The molecule in (B) was used to modulate a cholesteric LC droplet (a) and a plastic rod with a length of 28 µm and width of 5 µm (b). The helical axis of the cholesteric LC in the droplet was initially frustrated, forming a symmetric four-section optical texture. The texture rotated clockwise with 365 nm UV irradiation due to the change in the cell gap-to-pitch ratio; similarly, the plastic micro-rod rotated clockwise in the cholesteric system due to the change in cell gap-to-pitch ratio. D) The chiral molecular motor with only one rotor could be connected to the polymer chain, induced a helical polymer, and enabled handedness modulation with alternate UV and visible light irradiation through the chirality transformation. A) Reproduced with permission.[35] Copyright 2002, National Academy of Sciences, USA. B) Reproduced with permission.[43] Copyright 2008, American Chemical Society. C-a) Reproduced with permission.[41] Copyright 2014, The Royal Society of Chemistry; C-b) Reproduced with permission.[39] Copyright 2006, Springer Nature. D) Reproduced with permission.[42] Copyright 2008, American Chemical Society.

a (*P*,*P*)-*cis* isomer gradually under dark ambient conditions at 20 °C. Further irradiation with the same UV source triggered conformation to the (*M*,*M*)-*trans* form followed by recovery to the initial (*P*,*P*)-*trans* form upon heating the sample to 60 °C. Notably, the light-induced isomerization in this cycle was reversible; for instance, the (*M*,*M*)-*cis* isomer was transformed into the (*P*,*P*)-*trans* isomer by exposure using 380 nm or longer-wavelength light, and vice versa. However, the thermally induced transformation was irreversible (**Figure** 4A). The HTP of the initial (*P*,*P*)-*trans* state in the common LC E7 reached 69 μm^{-1} and decreased to 12 μm^{-1} as the conformation transformed into the (*P*,*P*)-*cis* state, enabling PBG modulation from the blue to red band for a system doped with 6.16 wt% chiral material.[35]

A second-generation chiral molecular motor, with heteroatoms as well as distinct rotors connected by C=C bonds, enabled ready control of the rotation direction by light (Figure 4B).[37–44] The single stereocenter on one rotor ensured unidirectional rotation of the rotor. The molecular structures of the motors were designed, synthesized, and adopted as chiral molecular dopants to modulate the PBG of the LC helical superstructure. However, a narrower spectral range from the green to red band was obtained due to the lower HTP of the chiral compound in the system. An intermediate state can be maintained by polymerizing photopolymerizable acrylate-based LCs.[37] Continuous optimization was implemented to increase the HTP in the LC solvent and to decrease the intrinsic high isomerization barrier, providing chirality recovery at room temperature without any other auxiliary external stimulation. Redshift of the PBG was observed over the entire visible spectral range upon 365 nm UV irradiation for 70 s, followed by thermal recovery at room temperature for about 33 min.[38] More interestingly, exotic light-manipulated rotation of a plastic micro-rod whose scale was about four orders of magnitude larger than the molecular size of the chiral motor was attained by controlling the surface chirality parameter determined by the HTP of the chiral motor (Figure 4C-b).[39] Additionally, the cholesteric droplet interfacial behaviors, such as coalescence and contact angle, as well as the corresponding changes in chiro-optical activity, were smoothly controlled by modulating the cell gap-to-pitch ratio (*d*/*P*) using a 365 nm UV source (Figure 4C-a).[41] Such a chiral motor with only one rotor was redesigned to substitute the terminal groups of helical macromolecules (polyisocyanate) covalently, which influenced the handedness of the macromolecules by controlling the chirality of the photoresponsive molecular motor moiety (Figure 4D).[42,43] The chiral molecular motor is thermostable and can be controlled alternately by irradiation with UV (365 nm) light and visible light (>480 nm). Further, such a macromolecular-scale chiral sense can be transmitted to larger-scale superstructures organized in a lyotropic cholesteric LC phase, confirming a chiral transformation from a nanoscale molecular size to a mesoscale macromolecular size and further to a microscale supramolecular assembly. The molecular design and synthesis regarding second-generation molecular motors have been explored in detail to improve the enantiomeric excess and to control the rotation direction of the motor.[44]

2.1.4. Helical LCs Containing Nanomaterials (Near-Infrared Response Helical LCs)

For convenient and safe application of photoresponsive chiro-optical devices, a light source with lower photon energy (i.e., longer output wavelength) is highly desirable and would lead to many other potential applications. Near-infrared (NIR) light is a satisfactory source due to its lower photon energy, lower damage, and higher penetration than UV and visible light, enabling fascinating applications in situations in which the latter two types of light are commonly unsuitable, such as material sensitizing, photocatalysis, and light therapy. However, it is challenging to use NIR light as a driving source since the energy of NIR photons is not strong enough to produce a transition from the ground state to an excited state. Thanks to the development of nanoscience in the last decade, which provided common materials with numerous unimaginable properties, additional opportunities for NIR-light-responsive chiro-optical soft materials have been created.[45,46] Upconversion nanoparticles (UCNPs), which have an unprecedented capability to convert NIR light into UV or visible light, are representative energy transducers for chiral materials. β-NaGdF$_4$-based core–shell UCNPs, which emit bluish visible light and UV light via irradiation with low- and high-intensity 980 nm NIR light, respectively (**Figure 5**A), were impregnated into an LC helical system containing azobenzene-based binaphthalene chiral additives to promote the interconversion between *trans*- and *cis*-conformations under alternate exposure of high- and low-intensity NIR light with the same wavelength.[47] Reversible PBG modulation spanning the blue, green, and red bands was first achieved simply by using an NIR source with different power intensities. In addition, core–multishell UCNPs with four shells (from inside to outside: NaYF$_4$; NaYF$_4$: Yb, Tm; NaYbF$_4$: Nd; NaYF$_4$) around the center of NaGdF$_4$: Yb, Er, which can absorb NIR light with two different wavelengths (808 and 980 nm) and perform conversion into UV and greenish visible light, respectively (Figure 5B), were obtained by advanced nanofabrication.[48] Thus, an NIR-triggered helical superstructure with handedness inversion was achieved in the system containing the aforementioned dithienylcyclopentene-based chiro-optical molecules, producing an NIR-light-manipulated chiro-optical soft helix in terms of both the pitch length and handedness for the first time. A similar reversible transformation between two helical superstructures with opposite handedness was observed as well.

On the other hand, metal nanoparticles such as gold nanoparticles normally generate surface plasma polariton resonance upon stimulation with light, producing a photothermal effect, heating the LC helical system, and finally resulting in modulation of the chiro-optical properties. The peak wavelength of the absorption band of a metal nanoparticle is approximately related to the size of the particles, which can be empirically expressed as $\lambda_{\max} = 95R + 420$,[49] where R is the aspect ratio of the nanoparticle and $\lambda_{\max}$ is the peak wavelength of the absorption band, which indicates that $\lambda_{\max}$ shifts to longer wavelengths only if R is increased. For instance, the peak wavelength of the absorption band can be shifted to 715 nm when the aspect ratio reaches ≈3.1 (i.e., nanorods), ensuring that the absorption band overlaps the NIR band. Recently, researchers intended to use gold nanorods (GNRs) as nanoscale heaters to increase the temperature of an LC helical system. To promote the dispersion of GNRs in LCs, the mesogenic surfactant was decorated on the surface to form a hydrophobic GNRs. The NIR-induced phase transition from the nematic to isotropic phase was achieved within 7 s in nematic LC E7 containing 0.2 wt% GNRs.[50] A similar strategy was also adopted to trigger handedness inversion of an LC helical superstructure with NIR by loading GNRs with an aspect ratio about 3.17 into an LC system containing a specific chiral material with thermally induced handedness inversion (Figure 5C).[51] With increasing temperature, the HTP of such chiral materials decreased and then increased, which enabled a PBG shift from a right-handed blue band, to a right-handed red band, an unwound state, another left-handed red band, and finally a left-handed blue band by continuous irradiation with 808 nm NIR light.

2.1.5. Photoresponsive Cubic BPLCs

Recently, sufficient research has been focused on another chiral-optical LC helical superstructure, that is, BPLCs with an exotic double-twisted helical superstructure (Figure 1B-b), and has rendered BPs a topic of common scientific interest. BPs can be divided into three sub-phases, that is, BPIII with an amorphous fluidic state and BPII and BPI, which have 3D self-organized cubic superstructures, where BPII is a simple cube and BPI is a body-centered cube. BPIII displays a fog-like texture, while BPII and BPI show colorful platelet textures determined by the lattice orientation.[52] The chiro-optical PBG effect of BPLCs is determined by the lattice orientation, that is, the Miller indices, h, k, and l; the lattice constant, a; and the average refractive index of the BP, $<n>$, and can be expressed as $\lambda_{\mathrm{M}} = \frac{2<n>a}{\sqrt{h^2+k^2+l^2}}$. Here, λ_{M} is the peak wavelength of the PBG, and the average refractive index is approximately $\frac{2n_{\mathrm{o}}+n_{\mathrm{e}}}{3}$, where n_{o} and n_{e} are the ordinary and extraordinary refractive indices of the LCs, respectively.[53] As a chiro-optical characteristic of BPLCs, the bandwidth of the PBG is generally narrower than that in the cholesteric phase (i.e., the aforementioned helical superstructure) due to the lattice effect; additionally, the reflectance is lower due to the random lattice orientation of the BP that results from the absence of surface anchoring on LC substrates. Therefore, the chiro-optical properties in randomly oriented BPs are weak and the corresponding applications are greatly restricted.

The prior work indicated that a homogenously oriented BP lattice had a much higher reflectance than a randomly oriented one and exhibited more obvious chiro-optical properties; however, such lattice orientation was not easy to achieve in a high-chirality LC system due to the defects that

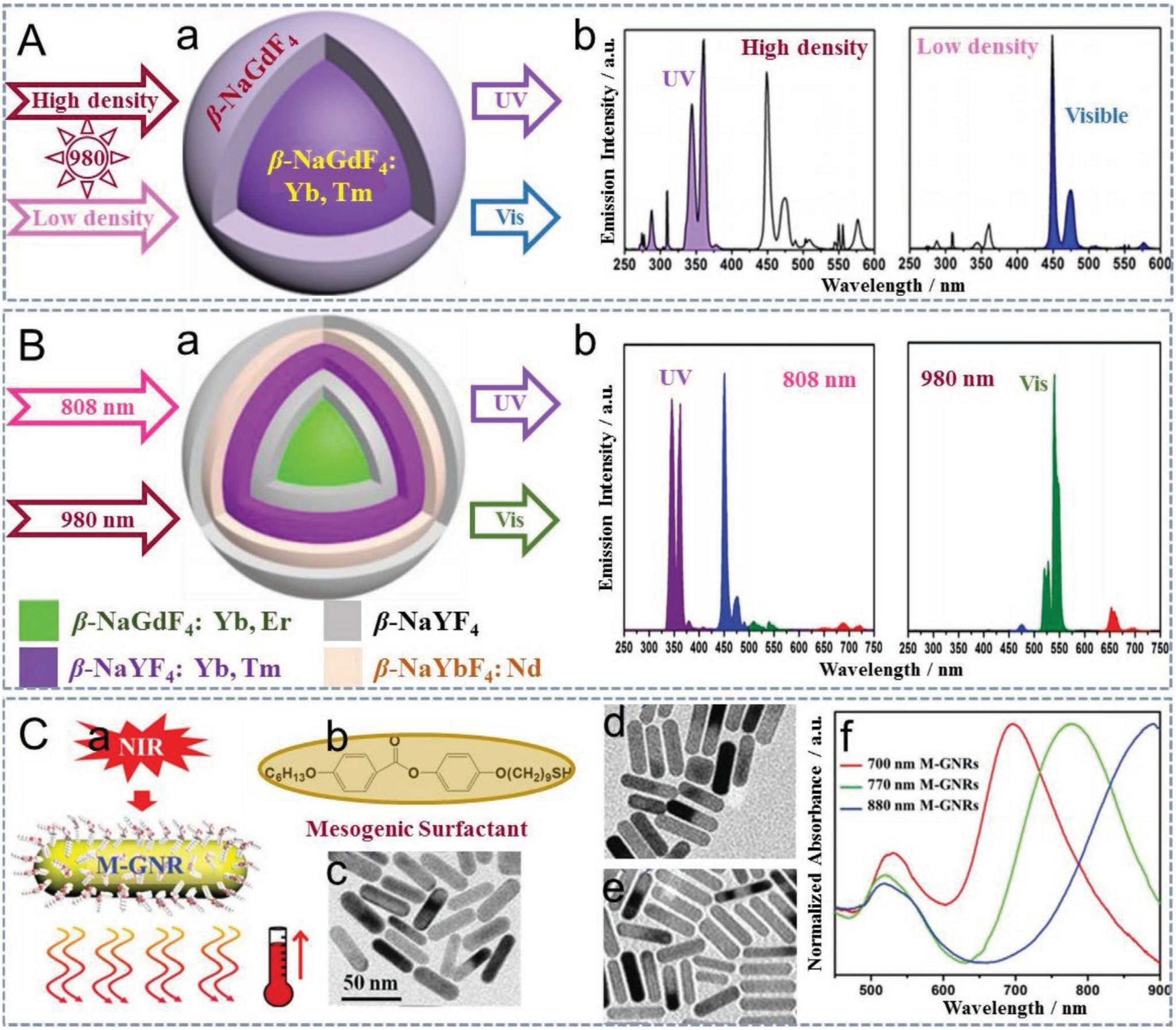

Figure 5. Nanomaterials used in photoresponsive helical LCs. A) Core–shell nanomaterial that is sensitive to the intensity of NIR light. a) The material emits UV and visible light upon irradiation with high- and low-intensity 980 nm light, respectively, as shown in the emission spectrum (b). B) Multi-core–shell nanomaterial that is sensitive to the wavelength of NIR light. a) The material emits UV and visible light upon irradiation with 808 nm and 980 nm NIR light, respectively, as displayed in the corresponding emission spectrum (b). C) A GNR exhibited a thermal effect upon irradiation with a certain NIR light, as schematically shown in (a). The nanorod surface was covered with a mesogenic surfactant (b) for better dispersion in LCs. The transmission electron microscopy (TEM) images display GNRs with a designed aspect ratio and absorption peaks at 700 nm (c), 770 nm (d), and 880 nm (e). The corresponding absorption spectra are shown in (f). A) Reproduced with permission.[47] Copyright 2014, American Chemical Society. B) Reproduced with permission.[48] Copyright 2015, Wiley-VCH. C) Reproduced with permission.[51] Copyright 2015, Wiley-VCH.

were inevitably generated and reduced the free energy of the whole system. Nevertheless, some impressive progress has been made on this topic in recent years. For instance, a mono-domain BP was induced by applying an alternating current (AC) electric field of 2 V μm^{-1} for 1 s, on account of the dielectric torque that enabled rearrangement of the BP lattice.[54] In addition, a large monocrystalline BP was developed using a gradient-temperature technique, forming a larger BP crystal with a lateral size of 1 cm and thickness of 100 μm that exhibited a much higher reflectance than the common polydomain BP.[55]

As innovative BPLCs distinct from the commonly adopted BP materials, photoresponsive BPLCs have recently attracted increasing interest due to their numerous advantages and provide an entirely different driving strategy using light.[56–63] The fundamental concept of such chiro-optical materials is based on the aforementioned photoresponsive chiral additives, which were doped properly into photo-irresponsive LCs, endowing the entire mixture with photoresponsiveness. However, the problem of a random lattice orientation leading to low reflectance and weak chiro-optical properties has still not been solved. A creative strategy was proposed by adopting photoresponsive

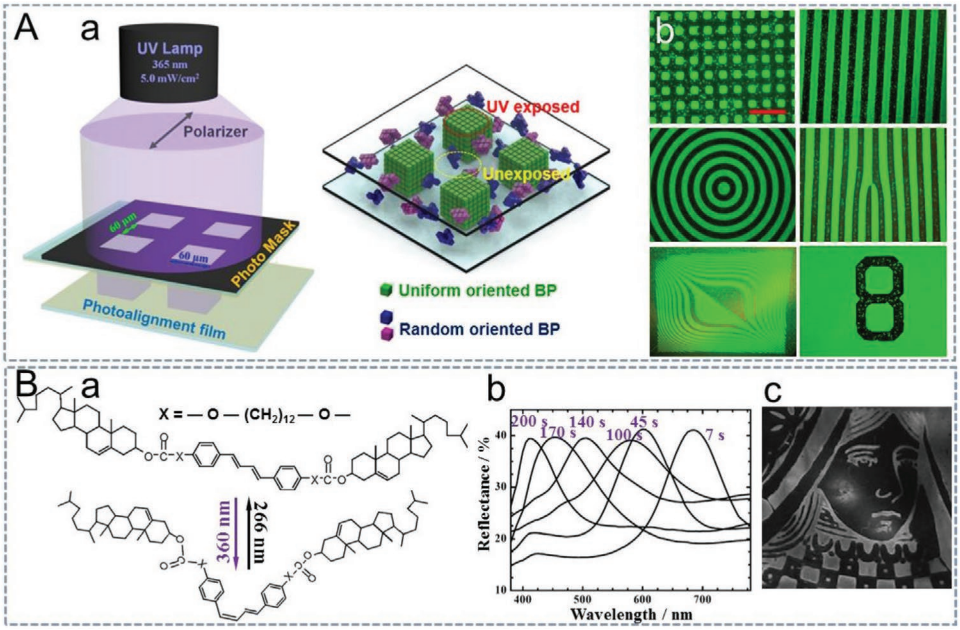

Figure 6. A) Photoresponsive cubic BPLCs produced by photoalignment. a) Patterned linearly polarized UV irradiation of photoalignment film coated on the inner surfaces of the cell substrates formed unidirectional alignment in the light-exposed square regions and resulted in a uniform crystallographic orientation of the BP lattice in the light-exposed regions and a random lattice orientation in the unexposed areas, enabling b) photo-writing of patterns due to the high reflection contrast between the uniform and randomly oriented BP regions. B-a) Diphenylbutadiene-based cholesteric LC, which exhibits interconversion photoisomerization upon irradiation by 360 nm (*trans*-to-*cis*) and 266 nm (*cis*-to-*trans*) sources. b) A blueshift of the PBG from the red to blue band was achieved by irradiation with 360 nm UV light, enabling c) image recording using light. A) Reproduced with permission.[65] Copyright 2017, Wiley-VCH. B) Reproduced with permission.[66] Copyright 2008, Wiley-VCH.

alignment film[64] to ensure a homogenous BP lattice orientation as well as a specific-patterned orientation with high resolution by irradiation with patterned light. The dominant mechanism was based on the mature photoalignment technique, that is, the LC planar orientation was controlled and programmed by the polarization direction of the light and was perpendicular to the polarization direction on the substrate surface.[65] Thus, micro-patterning was achieved readily by exposing the photoalignment film using a photomask, and correspondingly, the prescribed micro-patterns were written on the sample due to the selective local alignment (**Figure** 6A-a). Furthermore, such micro-patterns can be erased in situ by using a combination of uniform irradiation and a pulsed electric field and rewritten with patterned exposure. Micro-stripes, a square array, concentric circles, and other more complicated micro-patterns (Figure 6A-b) were written using light.

2.1.6. Another Type of Photoresponsive Helical LC

The development of LC chemistry in recent decades enhanced understanding of the arrangement, properties, and self-organized behavior and structure of LCs. A photoresponsive trimer helical LC with diphenylbutadiene linked to two cholesterols on either end via flexible alkoxy chains was synthesized, providing reversible PBG modulation covering the entire visible spectral band with alternate irradiation by 266 and 366 nm UV sources (Figure 6B-a,b).[66] Image recording was achieved, and storage was possible by converting the medium to a glassy state (Figure 6B-c).

Some LCs display intrinsic helicity owing to their specific molecular structures, such as ferroelectric and bent-core LCs, which exhibit periodic helices with helical pitches of several molecular scales.[67–69] Specifically, achiral twist-bend nematic (N_{tb}) LCs, which commonly have two rigid mesogenic moieties linked by a flexible hydrocarbon chain, show nematic orderliness but different self-organized arrangements and form helical superstructures of mesogenic moieties with helical pitches of several to tens of nanometers determined by the molecular structure.[70,71] However, in this progress report, we do not intend to demonstrate such helicity since the pitch length is much shorter than the scale of the wavelength of light; therefore, the chiro-optical effect of interest is quite weak in the UV to NIR bands. However, one exception, which is necessary and worth mentioning here, is the mixture of the N_{tb}LCs and common nematic LCs, which exhibited handedness-dependent PBG modulation in a wide spectral range from the UV band, through the entire visible band, to the NIR band driven by temperature or a weak AC electric field.[72–74] Such performance indicates a distinct LC arrangement (a heliconical arrangement) in the helical superstructure. That is, the molecular orientation is not perpendicular to the helical axis, but rather forms a certain angle with respect to this axis, generating a so-called oblique helix. The oblique angles of the LCs in the helix experience a dielectric torque from the applied electric field, decreasing the angles and thereby compressing the helical pitch. Theoretical investigations indicated a close dependence of the PBG modulation on the delicate equilibrium between the dielectric and elastic torques; in other words, the formation of a heliconical arrangement and the corresponding PBG modulation was determined by the ratio between the bend and twist elastic constants, K_{33}/K_{22}.[72]

A photoresponsive heliconical superstructure was recently proposed that was developed using a kind of N_{tb}LCs, denoted as CB7CB, and the commercial nematic LC mixture, E7. CB7CB has two cyanobiphenyl-based mesogenic moieties connected by an alkyl chain with seven carbons, which is a typical molecular structure possessing the N_{tb} phase.[71a] The commonly used chiral dopant R811 and photosensitive dithienylcyclopentene-based chiral materials previously mentioned were mixed together as the chiral agent. In each case, the contents were optimized to ensure both PBG modulation within a wide spectral range and satisfactory photoresponsiveness.[75] The results indicated continuous PBG modulation from the NIR band to the near-UV band as the applied electric field was reduced from 3.0 to 0.67 V μm^{-1}. Notably, the handedness of such heliconical superstructure can be inverted by external light stimulation, which changes the handedness-dependent PBG effect while retaining the wide dynamic spectral range of the PBG. Moreover, diverse micropatterns, such as periodic stripes and concentric circles, were generated through patterned exposure. Another interesting aspect that deserves mention is that the coexistence of two heliconical superstructures with opposite handedness and an unwound arrangement was formed via appropriate light exposure. Of course, the PBG effects in such systems were maintained, producing bright reflection colors that changed with the electric field.

2.2. Materials with Light-Modulated CD

CD is another important chiro-optical property for optically active materials, which generally displays a CPL handedness dependency on the absorption near the UV–visible absorption band of the chiro-optical medium caused by the asymmetric electron transitions of the medium. Distinct from the aforementioned PBG resulting from the effects of the self-organized microstructure on the photons, CD is attributable to the effects of the molecular structure on the electron transitions. Hence, similarly to UV–visible absorption, CD reflects electron movement in an optical manner. The CD of an optically active medium, displaying exciton splitting of the CD spectrum, can easily be qualitatively or quantitatively detected in situ through CD spectroscopy. The changes in the CD spectrum are inevitably correlated with the transformation of chiro-optical molecular conformation, enabling investigation of real-time molecular kinetics via analysis of the CD spectrum.[7] Herein, we focus on the CD and its modulation in some kinds of photoresponsive helical soft materials with mesogenic moieties in the molecules, that is, photoresponsive mesogenic helical soft materials, including polymers, LCs, and gels.

2.2.1. Photoresponsive Helical Polymers

Polymers with helical superstructures are typical chiro-optical materials exhibiting prominent CD, and have aroused increasing research interest over the past decades. Such chiral polymers normally include chiral segments in the backbone or side chains embedded via specific methodologies, such as metal-catalyzed polymerization, Suzuki–Miyaura coupling, and free radical polymerization. The photoresponse, however, is achieved by connecting the azobenzene derivatives, having both photosensitivity and mesogenic characteristics, in either the main or side chains. For instance, a series of photochromic polymethacrylates (PMAs) showing typical optical activity as well as conspicuous light-modulated CD were synthesized.[76–80] Such polymers commonly include photosensitive achiral rod-like mesogenic azobenzene moieties on their side chains (**Figure 7**A-a). A chiral amino acid group, such as left-handed alanine, leucine, valine, or proline,[76,77] with a carbon stereo-center and left-handed lactic[78,79] as well as appropriate comparability with the polymers, was interposed between the backbone and azobenzene moieties on the side chain to induce chirality of the compounds. This category of polymers exhibited optical chirality in both solutions and films due to asymmetric electron transitions, which subsequently induced a dipole interaction between two adjacent side chains, and hence presented exciton splitting of the CD spectrum. Irradiation by a UV source excited the photoisomerization of azobenzene moieties from the rod-shaped *trans*-conformation to bent *cis*-conformation as predicted, which disturbed the dipole interaction and thereby diminished the CD signal. Recovery can be promoted through irradiation by visible light since it triggers the *cis*-to-*trans* conversion of azobenzene moieties. Similar CD modulation was observed in both solutions and films, enabling the fabrication of a photocontrollable polymer CD switch. Here, it should be noted that the photoisomerization of azobenzene moieties in solid film was slightly hindered and hence influenced the photoisomerization rate and conversion. As mentioned previously, a prominent drawback of azobenzene is thermal instability, which inevitably leads to fatigue during the switching between UV and visible sources. Therefore, in a recent work, azobenzene was replaced with more stable spiropyran in the side chains of a PMA-based polymer (Figure 7A-b); the left-handed lactic was still interposed between the main chain and photosensitive groups to provide the polymer with optical chirality.[81] The synthesized polymer achieved significant thermal stability improvement, presenting a glass transition temperature around 100–130 °C and a decomposition temperature of 270 °C, without any negative influences on the capability of CD modulation by light. In addition, a dependency was observed between the optical chirality of the polymer and the number of lactic moieties in the polymer.

Some works have been focused on side-chain substituents of PMA-based polymers, where another azobenzene derivative, 4-cyanophenyl-3-carbazolyl diazene, was linked as the photosensitive moiety on the side chain instead of the common azobenzene, as mentioned above; likewise, the left-handed lactic provided the chirality of the formed homopolymer.[82–84] Such long conjugated cyanophenyl carbazolyl diazene moieties enhanced the dipole interactions of the side chains, facilitating the formation of chirality and producing a more obvious CD signal. The polymers (Figure 7A-c) in chloroform solution and solid film state exhibited apparent optical activity, with the Cotton effect reflected by the CD spectrum, which was switched on and off by alternating between UV and visible sources; thus, the requirements for potential CD switch applications

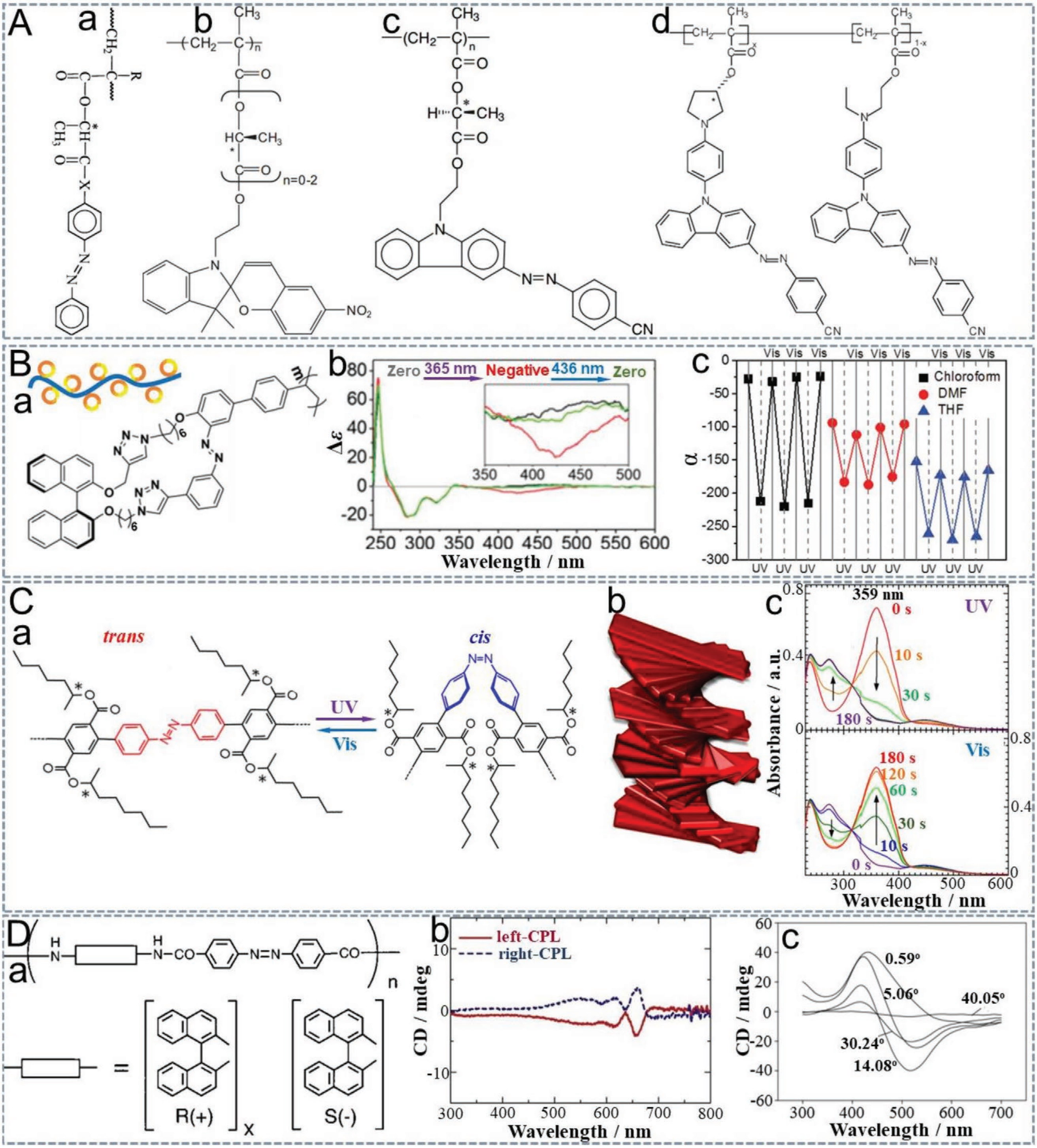

Figure 7. Photoresponsive helical polymers with CD effect. A) Series of PMA helical polymers bearing azobenzene (a), spiropyran (b), and cyanophenyl carbazolyl diazene (c,d). B) Polyvinyl-based homopolymers bearing cyclic pendent azobenzenophane groups (a) and corresponding CD modulation with alternating light irradiation (b,c): b) difference in absorbance ($\Delta\varepsilon$) between left- and right-handed CPL; c) optical rotation of the polymer during irradiation with alternating light. C-a) Polyazobenzene with interconversion between *trans*- and *cis*-conformations due to light exposure. b) Helical π-stacking model of molecules with *trans*-conformation and c) absorption in the UV–vis spectral range during irradiation with UV and visible light. D) Copolymers containing binaphthalene chiral moieties and photosensitive azobenzenes (a); CD spectra of helical polydiacetylene with left- and right-handedness formed by irradiation with left- and right-handed CPL, respectively (b); CD of an azobenzene polymer modulated by the ellipticity of an EPL (c). A-a) Reproduced with permission.[77] Copyright 2000, Wiley-VCH; A-b) Reproduced with permission.[81] Copyright 2012, Elsevier Ltd.; A-c) Reproduced with permission.[82] Copyright 2006, Wiley-VCH; A-d) Reproduced with permission.[83] Copyright 2009, Wiley-VCH. B) Reproduced with permission.[85] Copyright 2015, Royal Society of Chemistry. C) Reproduced with permission.[86] Copyright 2019, American Chemical Society. D-a) Reproduced with permission.[88] Copyright 2001, American Chemical Society; D-b) Reproduced with permission.[90] Copyright 2009, Elsevier Ltd.; D-c) Reproduced with permission.[91] Copyright 2006, Wiley-VCH.

were realized.[82] Furthermore, it was interesting to observe the optical refractive index modulation of the polymer upon irradiation by linearly polarized visible light due to the almost unidirectional self-organized arrangement of the anisotropic moieties in the side chains of the polymer (Figure 7A-d). Therefore, dynamic periodic phase-modulated grating was established via exposure of two interference laser beams.[83]

A judiciously designed polyvinyl-based homopolymer, bearing cyclic pendent azobenzenophane groups composed of photosensitive azobenzene and chiral binaphthalene moieties, was synthesized by free radical polymerization (Figure 7B-a).[85] The chirality of the polymer, resulting from the asymmetric geometry of azobenzenophanes, showed reversible light-modulated CD, from almost no signal (i.e., no optical chirality) initially to a negative signal (i.e., left-handed optical chirality), followed by recovery to the initial zero. This effect was produced by alternating between UV and visible irradiation (Figure 7B-b,c), due to the conspicuous *trans*-to-*cis* interconversion of the azobenzenophane groups. Notably, such CD modulation is potentially applicable to a light-driven chirality switch. Some researchers attempted to synthesize a photosensitive main-chain polymer to obtain a sufficient geometry change.[86] Polyazobenzenes with left-handed chiral substituents as the side chains were obtained via Suzuki–Miyaura coupling (Figure 7C-a). A helical superstructure of the polymer formed by molecular π stacking was also corroborated through the grazing incidence X-ray diffraction technique (Figure 7C-b). The azobenzene units transformed from a rectangular plate-like *trans*-isomer to a quadrate plate-like *cis*-isomer, when provided with UV (300–400 nm) irradiation; thus, the dipole interaction and optical chirality of the polymer were weakened.

On the other hand, polymers with the chiral moieties embedded into the backbone were deliberately designed. Polyketones, copolymerized by units of ketone and chiral spiroketal bearing azobenzene as the side groups, formed another photoresponsive optical chirality polymer, which exhibited modulation of the CD effect upon alternating irradiation with UV and visible light in chloroform.[87] As the polymer concentration was 0.19 mmol L^{-1}, the positive and negative Cotton bands in the ranges of 290–340 and 340–390 nm, respectively, almost disappeared after 1 h of irradiation by a high-pressure mercury lamp (spectral range: 320–420 nm) and recovered after at least 4 h of exposure to visible blue light. Moreover, a series of main-chain polymers containing both chiral binaphthalene and photosensitive azobenzene units was synthesized through solution polycondensation reactions at low temperature in a dark environment (Figure 7D-a).[88] The chirality, induced by binaphthalene units, was controlled by a UV lamp with a spectral peak around 360 nm. A gradual weakening of the CD effect was observed, due to the *trans*-to-*cis* isomerization, which probably sterically altered the dihedral angle between the two naphthalenes of the binaphthalene units and thereby induced a change in the asymmetric electron transitions. Optical chirality was recovered, accompanied by CD signal enhancement, under blue light irradiation with a spectral peak at 440 nm. Furthermore, excellent optical chirality inversion caused by the handedness inversion of the self-organized polymer helix was achieved by embedding the enantiomers of binaphthalene into the main chain of the polymer in a proper ratio. Specifically, a left- or right-handed helical superstructure can be induced in the main chain of polyazobenzene by hetero-aggregation with the enantiomeric pair of chiral polysilanes in the mixture.[89] The handedness and absorption can be modulated by light, as confirmed by the changes in the corresponding CD spectrum. CPL was also used to prepare a chiral polymer with the same handedness as the light.[90] The left- or right-handed chiral polydiacetylene was generated by photopolymerizing the photo-insensitive achiral pentacosadiynoic acid vapored monomers with the left- or right-handed CPL at a certain temperature, which facilitated the crystallization of the polymers (Figure 7D-b). In addition, the chirality and relevant CD effect of an epoxy-based amorphous achiral azobenzene polymer were induced and modulated by elliptically polarized light (EPL) (Figure 7D-c). The chirality and CD signal were respectively determined by the handedness and ellipticity of the EPL, which indicated that left-handed EPL induced a left-handed helix, and vice versa; furthermore, the intensity of the CD signal changed as the ellipticity of the EPL was reversed. Unlike the CD modulation of LC polymer by CPL, these modulations were caused by the preferential polarization direction of the EPL.[91]

2.2.2. Photoresponsive LC-Based Materials with Light-Modulated CD

Regarding LCs, the relevant PBG effect accompanied by light manipulation has been intensively explored; nevertheless, further attention is warranted regarding the CD behavior and its modulation in some elaborately designed LCs, such as some kinds of photoresponsive LC polymers and molecules with specific geometries. Photoresponsive azobenzene-based LC polymers have been fabricated and have witnessed rapid development in recent years, focusing on the photomechanical effect due to the significant geometric deformation of azobenzene derivatives during photoisomerization.[92–95] There have also been some impressive investigations of the CD effect, which has attracted increasing attention. A kind of LC copolymer with an acrylate-based backbone bearing azobenzene and cholesteryl units with an optimized ratio was spin-coated onto a substrate, forming a thin polymer film that showed a typical CD signal with a negative Cotton band corresponding to the π–π^* electron transition and a positive band owing to the n–π^* transition.[96] The negative band gradually disappeared with irradiation by 365 nm UV light and reached almost zero after about 100 s of exposure due to the phase transition from a self-organized helical superstructure to an isotropic state. Further exposure to 436 nm light caused the sample to enter an unexpected smectic phase, which can be recovered to the isotropic state by further UV stimulation; however, this phase cannot revert back to the original helical superstructure. Notably, intense light scattering was observed instead of the CD effect when the film was too thick, for example, 10 µm. Further molecular design regarding the pendant groups, such as the lateral substituents and terminal groups linked on azobenezene moieties, was implemented (**Figure** 8A).[97] The typical Cotton effect with a stronger CD signal was found in a thin film of the polymer having a lateral chlorine substituent on the pendant unit because the side units were more mobile, promoting self-organization to form a

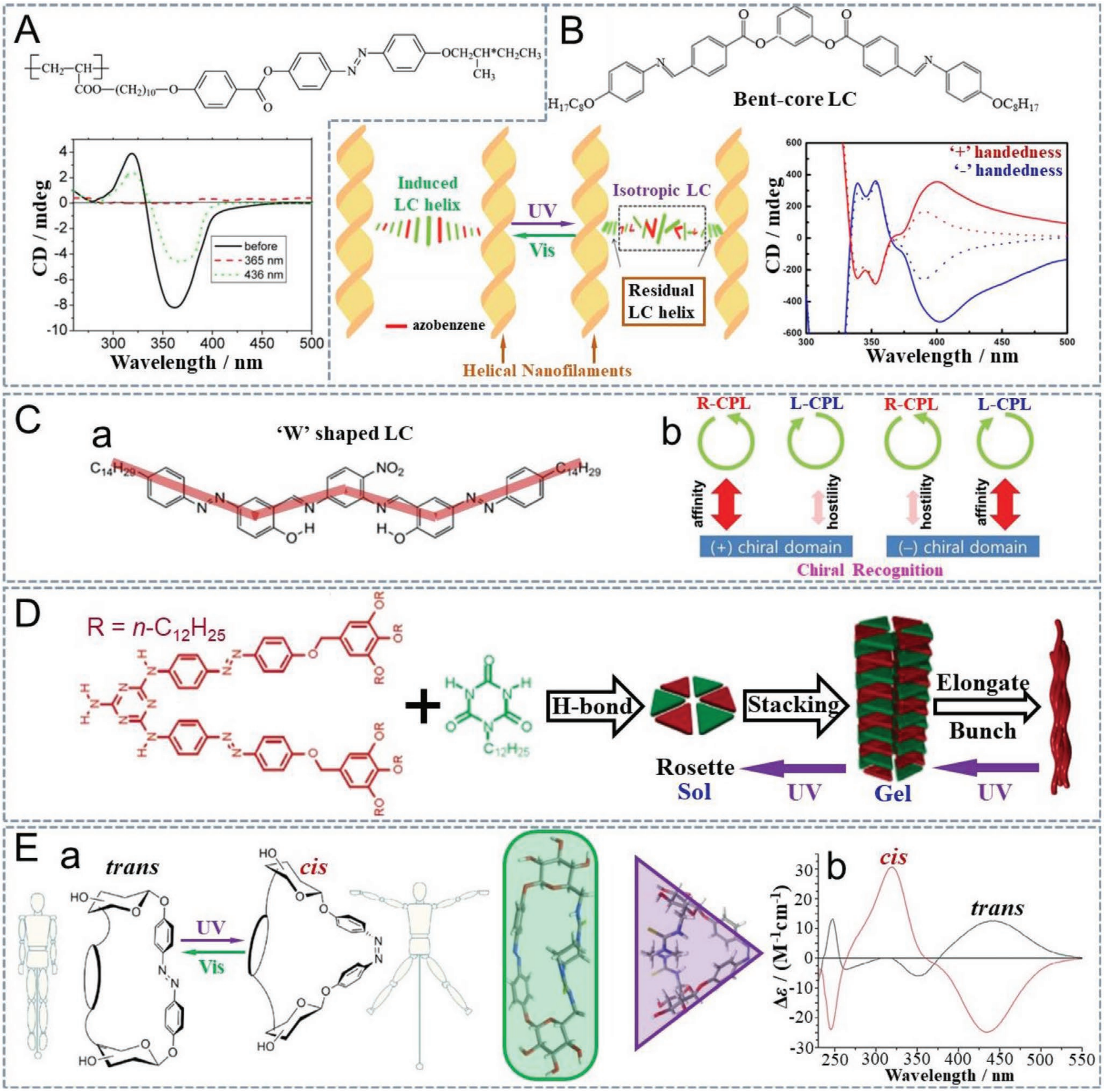

Figure 8. Photoresponsive helical LCs and gels with CD effect. A) Azobenzene-based LC polymer and corresponding CD spectra at initiation and after stimulation with 365 nm and 436 nm light. B) Bent-core helical nanofilaments induced helical arrangement of photoresponsive LCs, and the CD was modulated by UV irradiation. Solid line: initial CD spectrum; dotted line: CD spectrum after UV irradiation. C) Helical superstructure of the W-shaped LC (a), with handedness dependency on the incident CPL polarization (b). D) Stacking and fiber formation of a hydrogen-bonded rosette; and UV-modulated transformation from gel to sol. E-a) Macrocyclic glycoazobenzene with rectangular *trans*-conformation and triangular *cis*-conformation; b) difference in absorption of right- and left-handed CPL ($\Delta\varepsilon$) with respect to *trans*-isomers (black curve) and *cis*-isomers (red curve). A) Reproduced with permission.[97] Copyright 2013, American Chemical Society. B) Reproduced with permission.[99] Copyright 2015, American Chemical Society. C) Reproduced with permission.[100] Copyright 2016, Royal Society of Chemistry. D) Reproduced with permission.[101] Copyright 2005, American Chemical Society. E) Reproduced with permission.[104] Copyright 2017, Wiley-VCH.

regular helical superstructure. It also can be predicted that the CD signal can be switched on and off by alternating between 365 nm UV and 436 nm visible light (Figure 8A). In addition to photoresponsive LC polymers, some ingenious molecular structures of monomer LCs have been created, which have also exhibited excellent CD effects and light modulation. For example, a molecular crystal with two amphiphilic azobenzenes linked on either side of a chiral isosorbide via the flexible alkoxyl, possessing a liquid crystalline smectic A (SmA) phase, was found to have a helical self-organized superstructure in chloroform solution but no recognizable UV-induced CD changes.[98] However, by heating the material to an isotropic state and then cooling it to the SmA phase, discernable CD modulation with a concomitant geometric change from a helicoidal nanohelix to a flat nanobelt was achieved. This observation indicated that achiral bent-core LCs could form the helical superstructure via asymmetric dipole interactions, although a recent work additionally demonstrated an unprecedented helical superstructure of an achiral photoresponsive LC system induced by bent-core helical nanofilament (Figure 8B).[99] Such induced helices were reversibly unwound and reconfigured by alternating exposure with 365 nm UV and 450 nm visible light, producing light modulation of the CD effect and enabling the application of a light-driven CD switch. Optical chirality also can be modulated by altering the polarization of the light stimulus, that is, the irradiation of CPL with the same handedness as the chiral domains can increase the chirality, and vice versa (Figure 8C-a). Such superior performance was generated in a specifically designed W-shaped photosensitive LC having a unique smectic phase with segregated chiral domains (Figure 8C-b).[100] The reason for the polarization-dependent chirality can be considered to be an affinity between a chiral domain and CPL with the same handedness and hostility in the case of opposite handedness. Consequently, some potential applications, such as chiral sensors, chiral recognizers, and chiro-optical switches, have become much more realistic.

2.2.3. Photoresponsive Gels

The photoresponsive liquid crystalline gels formed by the hydrogen-bond self-organization between the barbiturate and azobenzene appended melamine were specifically investigated in terms of the mechanism and behavior of self-organization due to the exotic rosette structure.[101,103] The tridedocyloxyphenyl promoted steric stacking of the complexes to generate a columnar liquid crystalline gel in the bulky state, while such state was not observed in aliphatic solvent due to weakening of the aggregation. Therefore, the barbiturate component was replaced with *N*-dodecylcyanurate with enhanced steric stacking, resulting in a hexagonal columnar liquid crystalline gel in a face-to-face arrangement manner. An elongated helical fibrous state, formed in cyclohexane, can be triggered in the original gel state by UV light irradiation, and further exposure led to disorganization of the columnar state, inducing the transformation from gel to sol (Figure 8D).[101] The columnar liquid crystalline arrangement was re-established with visible light exposure. An amphiphilic chiral azobenzene-based gel was designed, connecting the long hydrophobic alkoxy on one side of azobenzene and the hydrophilic maltose or polyethyleneglycol (PEG) on the other side.[103] Left-handed phenylalanine was linked to provide the gel with chirality. The molecular weight of the terminal PEG determined the formation of gel in solutions, that is, a smaller molecular weight promoted the generation of the gel in either dimethylsulfoxide or aqueous solution; while a larger weight tended to form a fibrous helix in the water. In addition, a transition from gel to sol was triggered by UV irradiation due to the *trans*-to-*cis* photoisomerization of azobenzene, and thermal recovery of azobenzene led to the reappearance of gel. Gel recovery could be promoted by visible light exposure as well. Moreover, the azobenzene-based macrocyclic molecule was designed to change the optical chirality dramatically and to avoid multi-conformation of a single *trans*- or *cis*-isomer during photoisomerization.[104–107] Such macrocyclic materials were synthesized through cyclization between the azobenzene derivatives and chiral sugars (Figure 8E-a), which transferred the chirality to the mesogenic azobenzene moiety, enabling significant CD modulation of not only the absorption, but also the sign of the Cotton band (i.e., the chirality of the material) (Figure 8E-b). In addition, such macrocyclic materials exhibited the gel state in cyclohexane and ethanol, with interconversion between gel and sol through diverse stimuli, including light, temperature, and mechanical force. Another elaborate bolaamphiphile achiral azobenzene derivative with carboxyl-substituents exhibited specific head-to-head and side-by-side self-organized behavior via hydrogen bonds between two carboxylic acid groups to form a lamellar superstructure.[108] The helical nanotube could be formed in an acidic environment with a pH of 2.77 and became disorganized when the acidity was weakened due to the hydrogen-ion-impelled self-organization. Such helical nanotubes also can be unwound by UV irradiation and reconfigured by light exposure, accompanied by CD modulation attributable to the photoisomerization of azobenzene moieties.

2.3. Application Insights Based on Chiro-Optical Properties

A self-organized helical superstructure endows mesogenic soft materials with optical chirality caused by handedness-dependent refractive index modulation and light absorbance with respect to a certain incident CPL, producing two primary chiro-optical properties, PBG and CD, and consequently inspiring some categories of interesting photonic prototypes. Furthermore, in the development and growth of photosensitive materials, photoresponsiveness provides such soft materials with unprecedented vitality toward applications of light-modulated photonics and gradually has become the impetus for the thriving field of chiro-optics. Here, we will briefly demonstrate some kinds of photonic applications of broad interest based on photoresponsive self-organized helical mesogenic soft materials, such as diffraction gratings, laser emissions, and chiro-optical switches.

As mentioned previously, the PBG effect of a helical superstructure causes handedness-dependent selective reflection; in other words, light with the same wavelength as the PBG and the same handedness as the helix is completely reflected. A photoresponsive cholesteric LC (CLC) system containing azobenzene-based chiral molecular switches was exposed by patterned UV light, inducing a prescribed micro-pattern with binary selective reflection resulting from helical pitch elongation during the photoisomerization of chiral molecules in the exposed regions (**Figure 9**A-a).[109] Therefore, waveband-selective diffraction was generated when a CPL had both the same handedness as the CLCs and the same wavelength as the binary PBG (Figure 9A-b,c). Such waveband selectivity can be modulated by continuous irradiation of patterned light; for instance, green light can be diffracted by an original binary sample but not by a sample with

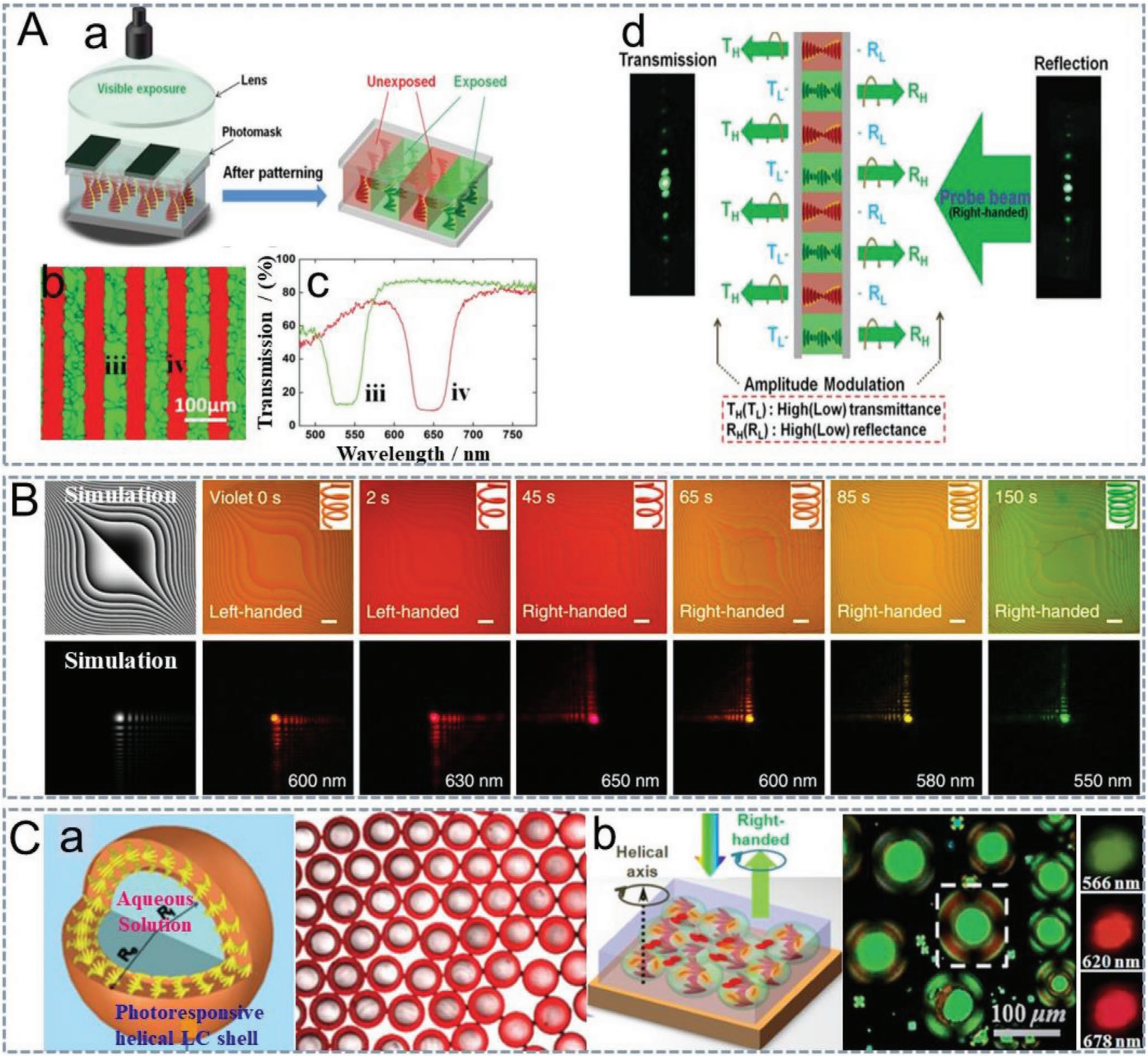

Figure 9. Photoresponsive chiro-optical applications. A) Waveband-selective diffraction grating generated by a) irradiation with a prescribed patterned light, forming b) periodic binary reflection stripes with c) two PBGs; d) periodic modulations of transmittance and reflectance were achieved on both sides of the sample. B) Helical LC-based planar reflective airy beam generator formed by photoalignment. Both the wavelength and handedness of the incident light, which can react with the pattern and produce an airy beam, can be modulated by light. C) Helical LC band-edge lasers emitted from the cavities of a microshell (c) and microdroplet (d). The emission wavelength can be modulated by light. A) Reproduced with permission.[109] Copyright 2016, Royal Society of Chemistry. B) Reproduced under the terms of the CC-BY Creative Commons Attribution 4.0 International License (http://creativecommons.org/licenses/by/4.0/).[113] Copyright 2019, The Authors, published by Springer Nature. C-a) Reproduced with permission.[121] Copyright 2014, Wiley-VCH; C-b) Reproduced with permission.[122] Copyright 2015, Royal Society of Chemistry.

the same pattern but a different binary PBG. The micro-pattern can be erased by irradiation with uniform visible light. In addition, diffraction interestingly occurred on both the reflection and transmission sides of the grating due to the amplitude modulation, which was a dominant reason for the light diffraction generated on each side (Figure 9A-d). Such a waveband-selective diffraction grating was also achieved in a photoresponsive LC copolymer bearing mesogenic azobenzene moieties[110] and a BPLC with periodic regional curing of the lattice crystallographic orientation.[65] Moreover, a CLC geometric phase related to CPL with a wavelength in the PBG was induced by an ingeniously designed orientation of LCs near the cell substrates via photoalignment.[111,112] This discovery facilitated recent progress in planar optical devices based on photoresponsive CLCs with handedness inversion. A reflective Airy beam generator was obtained, and the wavelength as well as the handedness of the incident CPL, which could produce the Airy beam, could easily be modulated by light due to the synchronous changes of the helical pitch length and handedness induced by the azobenzene-based chiral molecular switch utilized in the system (Figure 9B).[113]

The PBG of the helical mesogenic soft materials confines the motion of photons, resulting in a large density-of-state of photons at the edges of the PBG. As a proper amount of gain medium is dispersed homogeneously in a helical soft system and the fluorescent spectrum of the medium overlaps with the PBG, circularly polarized laser emission is generated at the band edges of the PBG in the case of external stimulation. The emission normally occurs at the long-wavelength band edge as less energy is needed for population inversion, which is the foundation of laser emission. The photoresponsiveness of a LC helical superstructure provides PBG modulation as well as handedness, enabling manipulation of both the emission wavelength and polarization and thus providing a possible material for all-optical controlling systems.[114,115] Azobenzene-based chiral molecular switches are always adopted in photoresponsive CLCs for light-manipulated laser emission considering the reversible modulation of the emission wavelength in a wide spectral range, although some other kinds of photosensitive materials have been used before, such as irreversible photopolymerizable[116] and photolytic[117] materials and photo-Fries transformation-based chiral materials.[118,119] Laser emission with reversible wavelength modulation in a spectral range wider than 100 nm was achieved in a CLC helical system containing a rod-like azobenzene derivative by alternately irradiating the system with UV and visible light.[120] The azobenzene-based binaphthalene chiral material was sufficiently impregnated into a spherical shell cavity provided by a CLC soft core–shell in a water/oil/water system, emitting an omnidirectional laser beam with a dynamic and reversible modulated wavelength upon UV and visible-light stimulation (Figure 9C-a).[121] To weaken the serious dependency of LC devices on cells, a mixture containing CLCs and aqueous polyvinyl alcohol solution was prepared and painted on a glass, cloth, or wood substrate. The painted film was dried at room temperature to form a film via deswelling of the mixture. As mentioned previously, a similar kind of azobenzene-based binaphthalene chiral material was premixed with CLCs to provide the film with photoresponsiveness, producing light-controllable laser emission with the wavelength shifted reversibly in the spectral range from 566 to 678 nm (Figure 9C-b).[122]

Another typical feature of photosensitive chiral molecules is CD accompanied by modulation via light irradiation. Some mesogenic soft materials containing photosensitive moieties and self-organized helical superstructures have exhibited excellent CD modulation, which will inevitably enable numerous promising chiro-optical applications. For instance, light-controllable photoswitching of CPL can be achieved by enhancing or weakening the absorption of the corresponding CPL through light exposure with a uniform intensity; moreover, any prescribed absorption-modulated diffraction pattern recorded, erased, and rewritten by light exposure can be achieved based on the mechanism of the CD effect, as mentioned above. A possible strategy for further enhancing the absorption could involve the use of an ingeniously designed metasurface[123,124] based on metal nanomaterials to generate a perfect absorber with tunable absorbance via a specific propagation behavior of surface plasma polaritons. To date, investigations related to chiro-optical applications based on CD modulation are insufficient, although this status does not mean that the field is in recession, but rather indicates the potential for considerable development and numerous application bottlenecks that demand prompt solutions.

3. Summary and Prospects

Chiral molecules, whose chirality transformations can induce the formation of helical architecture with a scale of several orders of magnitude larger than the molecular scale, constitute an exciting topic in chemistry, the materials sciences, and the biosciences. Such elegant helices, which are commonly established in mesogenic soft materials via molecular self-organization, have structural parameters with a scale comparable to that of the wavelength of light, thus exhibiting typical optical chirality effects and enabling diverse applications in chiro-optics. Photochromic chiral materials, which undergo prominent changes in molecular geometry due to photoisomerization, provide these soft helices with excellent photoresponsiveness, promoting the development of potential chiro-optical applications involving photoprogrammability.

The leveraging of light to control the self-organized structure of a soft superstructure or supramolecular assembly and hence to modulate the relevant chiro-optical properties provides numerous conceptual insights and innovative methods and has profound significance for both fundamental science and technological applications. However, the concomitant bottlenecks and scientific issues in the material design, synthesis, properties, device fabrication, and performance are formidable problems hindering further development. Nonetheless, extensive progress has been realized through improvements in materials, properties, and the relevant chiro-optical applications thanks to persistent research endeavors in recent decades, as described herein. For instance, the development of thermally stable and fatigue-resistant photochromic chiral molecular switches considerably enhanced the thermal stability compared with those of common photosensitive chiral materials; judicious material design generated significant CD modulation; and the intriguing chiro-optical diffraction and laser applications furnished unique attributes and optical performance. Further investigations can be focused on the design and synthesis of photochromic chiral materials with much higher thermal stability to achieve a soft helical system with reliable modulation by light. Simultaneously, the mechanism of the helix–photon interactions requires intensive study, and the structural design and modeling of chiro-optical devices with superior performance is inevitable. Overall, such work will serve not only as the foundation for future all-optical chiro-optical integration and systematization, but also will inspire insight and motivation toward other new properties and applications beyond optics.

Acknowledgements

The authors acknowledge the support from the National Key Research and Development Program of China (2017YFA0303700), the National Natural Science Foundation of China (NSFC) (Nos. 61822504, 51873060, 61575063, and 61435008), and the Shanghai Rising-Star Program (Grant No. 17QA1401100).

Conflict of Interest

The authors declare no conflict of interest.

Keywords

gels, liquid crystals, photoresponsive materials, polymers, soft materials

Received: August 16, 2019
Revised: February 24, 2020
Published online: June 2, 2020

---

[1] R. Bentley, *Chem. Soc. Rev.* **2005**, *34*, 609.
[2] F. Arnesano, A. Pannunzio, M. Coluccia, G. Natile, *Coord. Chem. Rev.* **2015**, *284*, 286.
[3] A. Broccolini, W. K. Engel, R. B. Alvarez, V. Askanas, *Am. J. Pathol.* **2000**, *156*, 1151.
[4] a) P. A. Korevaar, S. J. George, A. J. Markvoort, M. M. J. Smulders, P. A. J. Hilbers, A. P. H. J. Schenning, T. F. A. de Greef, E. W. Meijer, *Nature* **2012**, *481*, 492; b) R. Sun, X. Ma, M. Gao, H. Tian, Q. Li, *J. Am. Chem. Soc.* **2013**, *135*, 5990; c) H. Wang, H. K. Bisoyi, A. M. Urbas, T. J. Bunning, Q. Li, *Chem. - Eur. J.* **2019**, *25*, 1369.
[5] a) H. Kikuchi, in *Liquid Crystalline Functional Assemblies and Their Supramolecular Structures* (Ed: T. Kato), Springer, Berlin, Germany **2007**, Ch.3; b) R. S. Zola, Q. Li, in *Functional Organic and Hybrid Nanostructured Materials: Fabrication, Properties, and Applications* (Ed: Q. Li), Wiley-VCH, Weinheim, Germany **2018**, Ch.8; c) L. Wang, Q. Li, *Adv. Funct. Mater.* **2016**, *26*, 10; d) Z. Zheng, Q. Li, in *Nanomaterials for Sustainable Energy* (Ed: Q. Li), Springer, Heidelberg, Germany **2016**, Ch. 14; e) L. Wang, A. M. Urbas, Q. Li, *Adv. Mater.* **2019**, *31*, 1801335.
[6] Z. Chen, M. Segev, D. N. Christodoulides, *Rep. Prog. Phys.* **2012**, *75*, 086401.
[7] D. A. Leigh, E. M. Perez, *Supramolecular Chirality*, Springer-Verlag, Berlin, Germany **2006**.
[8] a) H. K. Bisoyi, Q. Li, in *Kirk-Othmer Encyclopedia of Chemical Technology*, John Wiley & Sons, New York **2014**, pp. 1–52; b) H. K. Bisoyi, T. J. Bunning, Q. Li, *Adv. Mater.* **2018**, *30*, 1706512; c) R. S. Zola, H. Bisoyi, H. Wang, A. Urbas, T. J. Bunning, Q. Li, *Adv. Mater.* **2019**, *31*, 1806172; d) L. Zhang, L. Wang, U. S. Hiremath, H. K. Bisoyi, G. C. Nair, C. V. Yelamaggad, A. M. Urbas, T. J. Bunning, Q. Li, *Adv. Mater.* **2017**, *29*, 1700676; e) L. Wang, H. K. Bisoyi, Z. Zheng, K. G. Gutierrez-Cuevas, G. Singh, S. Kumar, T. J. Bunning, Q. Li, *Mater. Today* **2017**, *20*, 230; f) K. G. Gutierrez-Cuevas, L. Wang, Z. Zheng, H. K. Bisoyi, G. Li, L. Tan, R. A. Vaia, Q. Li, *Angew. Chem., Int. Ed.* **2016**, *55*, 13090.
[9] H. K. Bisoyi, Q. Li, *Chem. Rev.* **2016**, *116*, 15089.
[10] S. Toksoz, H. Acar, M. O. Guler, *Soft Matter* **2010**, *6*, 5839.
[11] a) *Photoactive Functional Soft Materials: Preparation, Properties, and Applications* (Ed: Q. Li), Wiley-VCH, Weinheim, Germany **2019**; b) L. Wang, Q. Li, *Chem. Soc. Rev.* **2018**, *47*, 1044.
[12] a) Y. Li, M. Wang, T. J. White, T. J. Bunning, Q. Li, *Angew. Chem., Int. Ed.* **2013**, *52*, 8925; b) L. Ma, W. Hu, Z. Zheng, S. Wu, P. Chen, Q. Li, Y. Lu, *Adv. Opt. Mater.* **2019**, *7*, 1900393.
[13] M. Moriyama, N. Mizoshita, T. Yokota, K. Kishimoto, T. Kato, *Adv. Mater.* **2003**, *15*, 1335.
[14] a) Q. Li, L. Li, J. Kim, H. Park, J. Williams, *Chem. Mater.* **2005**, *17*, 6018; b) L. Green, Y. Li, T. White, A. Urbas, T. Bunning, Q. Li, *Org. Biomol. Chem.* **2009**, *7*, 3930.
[15] T. Ikeda, *J. Mater. Chem.* **2003**, *13*, 2037.
[16] R. Eelkema, B. L. Feringa, *Org. Biomol. Chem.* **2006**, *4*, 3729.
[17] a) S. Pieraccini, S. Masiero, A. Ferrarini, G. P. Spada, *Chem. Soc. Rev.* **2011**, *40*, 258; b) Y. Wang, Q. Li, *Adv. Mater.* **2012**, *24*, 1926; c) M. Mathews, N. Tamaoki, *J. Am. Chem. Soc.* **2008**, *130*, 11409; d) Y. Kim, N. Tamaoki, *Chem. Photo. Chem.* **2019**, *3*, 284; e) H. Wang, H. K. Bisoyi, M. E. McConney, A. M. Urbas, T. J. Bunning, Q. Li, *Adv. Mater.* **2019**, *31*, 1902958.
[18] H. K. Bisoyi, Q. Li, *Acc. Chem. Res.* **2014**, *47*, 3184.
[19] a) Q. Li, L. Green, N. Venkataraman, I. Shiyanovskaya, A. Khan, A. Urbas, J. W. Doane, *J. Am. Chem. Soc.* **2007**, *129*, 12908; b) T. J. White, R. L. Bricker, L. V. Natarajan, N. V. Tabiryan, L. Green, Q. Li, T. J. Bunning, *Adv. Funct. Mater.* **2009**, *19*, 3484; c) N. Venkataraman, G. Magyar, E. Montbach, A. Khan, T. Schneider, J. W. Doane, L. Green, Q. Li, *J. Soc. Inf. Disp.* **2009**, *17*, 869.
[20] a) J. Li, H. Bisoyi, J. Tian, J. Guo, Q. Li, *Adv. Mater.* **2019**, *31*, 1807751; b) J. Li, H. K. Bisoyi, S. Lin, J. Guo, Q. Li, *Angew. Chem., Int. Ed.* **2019**, *58*, 16052.
[21] J. Ma, Y. Li, T. White, A. Urbas, Q. Li, *Chem. Commun.* **2010**, *46*, 3463.
[22] Q. Li, Y. Li, J. Ma, D. K. Yang, T. J. White, T. J. Bunning, *Adv. Mater.* **2011**, *23*, 5069.
[23] Y. Wang, A. Urbas, Q. Li, *J. Am. Chem. Soc.* **2012**, *134*, 3342.
[24] H. Wang, H. K. Bisoyi, A. Urbas, T. J. Bunning, Q. Li, *J. Am. Chem. Soc.* **2019**, *141*, 8078.
[25] H. Wang, H. K. Bisoyi, L. Wang, A. Urbas, T. J. Bunning, Q. Li, *Angew. Chem., Int. Ed.* **2018**, *57*, 1627.
[26] a) Y. Li, A. Urbas, Q. Li, *J. Am. Chem. Soc.* **2012**, *134*, 9573; b) Y. Li, M. Wang, A. Urbas, Q. Li, *J. Mater. Chem. C* **2013**, *1*, 3889; c) Y. Li, Q. Li, *Org. Lett.* **2012**, *14*, 4362; d) Y. Li, M. Wang, H. Wang, A. Urbas, Q. Li, *Chem. - Eur. J.* **2014**, *20*, 16286.
[27] a) T. van Leeuwen, T. C. Pijper, J. Areephong, B. L. Feringa, W. R. Browne, N. Katsonis, *J. Mater. Chem.* **2011**, *21*, 3142; b) K. Rameshbabu, A. Urbas, Q. Li, *J. Phys. Chem. B* **2011**, *115*, 3409; c) Y. Li, A. Urbas, Q. Li, *J. Org. Chem.* **2011**, *76*, 7148.
[28] J. Fan, Y. Li, H. K. Bisoyi, R. S. Zola, D. K. Yang, T. J. Bunning, D. A. Weitz, Q. Li, *Angew. Chem., Int. Ed.* **2015**, *54*, 2160.
[29] Y. Li, C. Xue, M. Wang, A. Urbas, Q. Li, *Angew. Chem., Int. Ed.* **2013**, *52*, 13703.
[30] H. K. Bisoyi, Q. Li, *Angew. Chem., Int. Ed.* **2016**, *55*, 2994.
[31] Z. Zheng, Y. Li, H. K. Bisoyi, L. Wang, T. J. Bunning, Q. Li, *Nature* **2016**, *531*, 352.
[32] Z. Zheng, R. S. Zola, H. K. Bisoyi, L. Wang, Y. Li, T. J. Bunning, Q. Li, *Adv. Mater.* **2017**, *29*, 1701903.
[33] M. Mathews, R. S. Zola, S. Hurley, D. K. Yang, T. J. White, T. J. Bunning, Q. Li, *J. Am. Chem. Soc.* **2010**, *132*, 18361.
[34] B. L. Feringa, R. A. van Delden, N. Koumura, E. M. Geertsema, *Chem. Rev.* **2000**, *100*, 1789.
[35] R. A. van Delden, N. Koumura, N. Harada, B. L. Feringa, *Proc. Natl. Acad. Sci. USA* **2002**, *99*, 4945.
[36] T. van Leeuwen, A. S. Lubbe, P. Štacko, S. J. Wezenberg, B. L. Feringa, *Nat. Rev. Chem.* **2017**, *1*, 0096.
[37] R. A. van Delden, M. B. van Gelder, N. P. M. Huck, B. L. Feringa, *Adv. Funct. Mater.* **2003**, *13*, 319.
[38] R. Eelkema, B. L. Feringa, *Chem. - Asian J.* **2006**, *1*, 367.
[39] R. Eelkema, M. M. Pollard, J. Vicario, N. Katsonis, B. S. Ramon, C. W. M. Bastiaannsen, D. J. Broer, B. L. Feringa, *Nature* **2006**, *440*, 163.
[40] S. J. Aβhoff, S. Lamsaard, A. Bosco, J. J. L. M. Cornelissen, B. L. Feringa, N. Katsonis, *Chem. Commun.* **2013**, *49*, 4256.
[41] J. Chen, E. Lacaze, E. Brasselet, S. R. Harutyunyan, N. Katsonis, B. L. Feringa, *J. Mater. Chem. C* **2014**, *2*, 8137.
[42] D. Pijper, M. G. M. Jongejan, A. Meetsma, B. L. Feringa, *J. Am. Chem. Soc.* **2008**, *130*, 4541.
[43] A. Bosco, M. G. M. Jongejan, R. Eelkema, N. Katsonis, E. Lacaze, A. Ferrarini, B. L. Feringa, *J. Am. Chem. Soc.* **2008**, *130*, 14615.

[44] T. C. Pijper, D. Pijper, M. M. Pollard, F. Dumur, S. G. Davey, A. Meetsma, B. L. Feringa, *J. Org. Chem.* **2010**, *75*, 825.
[45] a) G. Chen, H. Qiu, P. N. Prasad, X. Chen, *Chem. Rev.* **2014**, *114*, 5161; b) H. Bisoyi, A. Urbas, Q. Li, *Adv. Opt. Mater.* **2018**, *6*, 1800458.
[46] a) *Anisotropic Nanomaterials: Preparation, Properties, and Applications* (Ed: Q. Li), Springer, Heidelberg, Germany **2015**; b) J. Zhou, Q. Liu, W. Feng, Y. Sun, F. Li, *Chem. Rev.* **2015**, *115*, 395; c) C. Xue, Q. Li, in *Encyclopedia of Surface and Colloid. Science* (Ed: P. Somasundaran), Taylor & Francis, Boca Raton, FL, USA **2015**.
[47] L. Wang, H. Dong, Y. Li, C. Xue, L. D. Sun, C. H. Yan, Q. Li, *J. Am. Chem. Soc.* **2014**, *136*, 4480.
[48] L. Wang, H. Dong, Y. Li, R. Liu, Y. F. Wang, H. K. Bisoyi, L. D. Sun, C. H. Yan, Q. Li, *Adv. Mater.* **2015**, *27*, 2065.
[49] C. Xue, Q. Li, in *Anisotropic Nanomaterials: Preparation, Properties, and Applications* (Ed: Q. Li), Springer, Heidelberg, Germany **2015**, Ch.3.
[50] K. G. Gutierrez-Cuevas, L. Wang, C. Xue, G. Singh, S. Kumar, A. Urbas, Q. Li, *Chem. Commun.* **2015**, *51*, 9845.
[51] L. Wang, K. G. Gutierrez-Cuevas, A. Urbas, Q. Li, *Adv. Opt. Mater.* **2016**, *4*, 247.
[52] a) D. C. Wright, N. D. Mermin, *Rev. Mod. Phys.* **1989**, *61*, 385; b) T.-H. Lin, C.-W. Chen, Q. Li, in *Anisotropic Nanomaterials: Preparation, Properties, and Applications* (Ed: Q. Li), Springer, Heidelberg, Germany **2015**, Ch.9.
[53] D. K. Yang, S. T. Wu, *Fundamentals of Liquid Crystal Devices*, John Wiley & Sons, New York **2012**.
[54] Y. Chen, S. T. Wu, *Appl. Phys. Lett.* **2013**, *102*, 171110.
[55] C. W. Chen, C. T. Hou, C. C. Li, H. C. Jau, C. T. Wang, C. L. Hong, D. Y. Guo, C. Y. Wang, S. P. Chiang, T. J. Bunning, I. C. Khoo, T. H. Lin, *Nat. Commun.* **2017**, *8*, 727.
[56] A. Chanishvili, G. Chilaya, G. Petriashvili, P. J. Collings, *Phys. Rev. E* **2005**, *71*, 051705.
[57] H. Y. Liu, C. T. Wang, C. Y. Hsu, T. H. Lin, J. H. Liu, *Appl. Phys. Lett.* **2010**, *96*, 121103.
[58] Y. Wen, Z. Zheng, H. Wang, D. Shen, *Liq. Cryst.* **2012**, *39*, 509.
[59] M. J. Gim, S. T. Hur, K. W. Park, M. Lee, S. W. Choi, H. Takezoe, *Chem. Commun.* **2012**, *48*, 9968.
[60] Y. Wu, Y. Zhou, L. Yin, G. Zou, Q. Zhang, *Liq. Cryst.* **2013**, *40*, 726.
[61] T. H. Lin, Y. Li, C. T. Wang, H. C. Jau, C. W. Chen, C. C. Li, H. K. Bisoyi, T. J. Bunning, Q. Li, *Adv. Mater.* **2013**, *25*, 5050.
[62] M. Wang, W. Hu, L. Wang, D. Y. Guo, T. H. Lin, L. Zhang, H. Yang, *J. Mater. Chem. C* **2018**, *6*, 7740.
[63] K. Zhou, H. K. Bisoyi, J. Q. Jin, C. L. Yuan, Z. Liu, D. Shen, Y. Q. Lu, Z. G. Zheng, W. A. Zhang, Q. Li, *Adv. Mater.* **2018**, *30*, 1800237.
[64] V. G. Chigrinov, V. M. Kozenkov, H. S. Kwok, *Photoalignment of Liquid Crystalline Materials: Physics and Applications*, John Wiley & Sons, Chichester, UK **2008**.
[65] Z. G. Zheng, C. L. Yuan, W. Hu, H. K. Bisoyi, M. J. Tang, Z. Liu, P. Z. Sun, W. Q. Yang, X. Q. Wang, D. Shen, Y. Li, F. F. Ye, Y. Q. Lu, G. Li, Q. Li, *Adv. Mater.* **2017**, *29*, 1703165.
[66] R. K. Vijayaraghavan, S. Abraham, H. Akiyama, S. Furumi, N. Tamaoki, S. Das, *Adv. Funct. Mater.* **2008**, *18*, 2510.
[67] L. E. Hough, N. A. Clark, *Phys. Rev. Lett.* **2005**, *95*, 107802.
[68] L. E. Hough, C. Zhu, M. Nakata, N. Chattham, G. Dantlgraber, C. Tschierske, N. A. Clark, *Phys. Rev. Lett.* **2008**, *101*, 079802.
[69] M. Mathews, R. Zola, D. Yang, Q. Li, *J. Mater. Chem.* **2011**, *21*, 2098.
[70] C. Meyer, G. R. Luckhurst, I. Dozov, *Phys. Rev. Lett.* **2013**, *111*, 067801.
[71] a) V. Borshch, Y. K. Kim, J. Xiang, M. Gao, A. Jákli, V. P. Panov, J. K. Vij, C. T. Imrie, M. G. Tamba, G. H. Mehl, O. D. Lavrentovich, *Nat. Commun.* **2013**, *4*, 2635; b) Y. Wang, G. Singh, D. M. Agra-Kooijman, M. Gao, H. K. Bisoyi, C. Xue, M. Fisch, S. Kumar, Q. Li, *CrystEngComm* **2015**, *17*, 2778.
[72] Z. Parsouzi, S. M. Shamid, V. Borshch, P. K. Challa, A. R. Baldwin, M. G. Tamba, C. Welch, G. H. Mehl, J. T. Gleeson, A. Jákli, O. D. Lavrentovich, D. W. Allender, J. V. Selinger, S. Sprunt, *Phys. Rev. X* **2016**, *6*, 021041.
[73] J. Xiang, S. V. Shiyanovskii, C. Inrie, O. D. Lavrentovich, *Phys. Rev. Lett.* **2014**, *112*, 217801.
[74] a) Y. Wang, Z. Zheng, H. K. Bisoyi, K. G. Gutierrez-Cuevas, L. Wang, R. S. Zola, Q. Li, *Mater. Horiz.* **2016**, *3*, 442; b) J. Xiang, Y. Li, Q. Li, D. A. Patersonn, J. M. D. Storey, C. T. Imrie, O. D. Lavrentovich, *Adv. Mater.* **2015**, *27*, 3014.
[75] C. L. Yuan, W. Huang, Z. G. Zheng, B. Liu, H. K. Bisoyi, Y. Li, D. Shen, Y. Q. Lu, Q. Li, *Sci. Adv.* **2019**, *5*, eaax9501.
[76] A. Altomare, R. Solaro, L. Angiolini, D. Caretti, C. Carlini, *Polymer* **1995**, *36*, 3819.
[77] C. Carlini, A. Fissi, A. M. R. Galletti, G. Sbrana, *Macromol. Chem. Phys.* **2000**, *201*, 1161.
[78] L. Angiolini, D. Caretti, L. Giorgini, E. Salatelli, A. Altomare, C. Carlini, R. Solaro, *Polymer* **2000**, *41*, 4767.
[79] L. Angiolini, D. Caretti, L. Giorgini, E. Salatelli, A. Altomare, C. Carlini, R. Solaro, *Polymer* **1998**, *39*, 6621.
[80] L. Angiolini, T. Benelli, L. Giorgini, *Macromol. Chem. Phys.* **2007**, *208*, 2348.
[81] L. Angiolini, T. Benelli, E. Bicciocchi, L. Giorgini, F. M. Raymo, *React. Funct. Polym.* **2012**, *72*, 469.
[82] L. Angiolini, T. Benelli, L. Giorgini, F. Mauriello, E. Salatelli, *Macromol. Chem. Phys.* **2006**, *207*, 1805.
[83] L. Angiolini, L. Giorgini, F. Mauriello, P. Rochon, *Macromol. Chem. Phys.* **2009**, *210*, 77.
[84] L. Angiolini, T. Benelli, L. Giorgini, A. Golemme, L. Mazzocchetti, R. Termine, *Dyes Pigm.* **2014**, *102*, 53.
[85] J. Liu, G. Jiang, Z. Zhang, W. Zhang, Y. Yang, Y. Wang, N. Zhou, X. Zhu, *Polym. Chem.* **2015**, *6*, 8144.
[86] M. Otaki, R. Kumai, H. Sagayama, H. Goto, *Macromolecules* **2019**, *52*, 2340.
[87] N. Kosaka, T. Oda, T. Hiyama, K. Nozaki, *Macromolecules* **2004**, *37*, 3159.
[88] S. R. Lustig, G. J. Everlof, G. D. Jaycox, *Macromolecules* **2001**, *34*, 2364.
[89] H. Chen, L. Yin, M. Liu, L. Wang, M. Fujiki, W. Zhang, X. Zhu, *RSC Adv.* **2019**, *9*, 4849.
[90] H. Kohn, T. Shino, Y. Ohshima, T. Manaka, M. Iwamoto, *Thin Solid Films* **2009**, *518*, 842.
[91] M. J. Kim, S. J. Yoo, D. Y. Kim, *Adv. Funct. Mater.* **2006**, *16*, 2089.
[92] H. Yu, Q. Li, in *Intelligent Stimuli Responsive Materials: From Well-defined Nanostructures to Applications* (Ed: Q. Li), John Wiley & Sons, Hoboken, NJ, USA **2013**, Ch.7.
[93] C. J. Barrett, J. Mamiya, K. G. Yager, T. Ikeda, *Soft Matter* **2007**, *3*, 1249.
[94] H. F. Yu, T. Ikeda, *Adv. Mater.* **2011**, *23*, 2149.
[95] L. Yu, H. Yu, Q. Li, in *Nanoscience with Liquid Crystals: From Self-Organized Nanostructures to Applications* (Ed: Q. Li), Springer, Heidelberg, Germany **2014**, Ch. 10.
[96] A. Bobrovsky, V. Shibaev, *J. Photochem. Photobiol. A: Chem.* **2005**, *172*, 140.
[97] A. Bobrovsky, V. Shibaev, A. Bubnov, V. Hamplová, M. Kašpar, M. Glogarová, *Macromolecules* **2013**, *46*, 4276.
[98] D. Y. Kim, W. J. Yoon, Y. J. Choi, S. I. Lim, J. Koo, K. J. Jeong, *J. Mater. Chem. C* **2018**, *6*, 12314.
[99] K. Kim, H. Kim, S. Y. Jo, F. Araoka, D. K. Yoon, S. W. Choi, *ACS Appl. Mater. Interfaces* **2015**, *7*, 22686.
[100] S. W. Choi, H. Takezoe, *Soft Matter* **2016**, *12*, 7937.
[101] S. Yagai, T. Nakajima, K. Kishikawa, S. Kohmoto, T. Karatsu, A. Kitamura, *J. Am. Chem. Soc.* **2005**, *127*, 11134.
[102] S. Yagai, T. Nakajima, T. Karatsu, K. Saiytow, A. Kitamura, *J. Am. Chem. Soc.* **2004**, *126*, 11500.

[103] M. J. Clemente, R. M. Tejedor, P. Romero, J. Fitremann, L. Oriol, *New J. Chem.* **2015**, *39*, 4009.
[104] G. Despras, J. Hain, S. O. Jaeschke, *Chem. - Eur. J.* **2017**, *23*, 10838.
[105] C. Lin, S. Maisonneuve, R. Métivier, J. Xie, *Chem. - Eur. J.* **2017**, *23*, 14996.
[106] K. Takaishi, M. Kawamoto, K. Tsubaki, T. Furuyama, A. Muranaka, M. Uchiyama, *Chem. - Eur. J.* **2011**, *17*, 1778.
[107] K. Takaishi, M. Kawamoto, *Molecules* **2011**, *16*, 1603.
[108] Q. Hu, Y. Wang, J. Jia, C. Wang, L. Feng, R. Dong, X. Sunn, J. Hao, *Soft Matter* **2012**, *8*, 11492.
[109] P. Z. Sun, Z. Liu, W. Wang, L. L. Ma, D. Shen, W. Hu, Y. Q. Lu, L. Chen, Z. G. Zheng, *J. Mater. Chem. C* **2016**, *4*, 9325.
[110] A. Ryabchun, A. Bobrovsky, Y. Gritsai, O. Sakhno, V. Shibaev, J. Stumpe, *ACS Appl. Mater. Interfaces* **2015**, *7*, 2554.
[111] J. Kobashi, H. Yoshida, M. Ozaki, *Nat. Photonics* **2016**, *10*, 389.
[112] J. Kobashi, H. Yoshida, M. Ozaki, *Phys. Rev. Lett.* **2016**, *116*, 253903.
[113] P. Chen, L. L. Ma, W. Hu, Z. X. Shen, H. K. Bisoyi, S. B. Wu, S. J. Ge, Q. Li, Y. Q. Lu, *Nat. Commun.* **2019**, *10*, 2518.
[114] H. Coles, S. Morris, *Nat. Photonics* **2010**, *4*, 676.
[115] A. D. Ford, S. M. Morris, H. J. Coles, *Mater. Today* **2006**, *9*, 36.
[116] A. Y. G. Fuh, T. H. Lin, J. H. Liu, F. C. Wu, *Opt. Express* **2004**, *12*, 1857.
[117] S. Furumi, S. Yokoyama, A. Otomo, S. Mashiko, *Appl. Phys. Lett.* **2004**, *84*, 2491.
[118] A. Chanishvili, G. Chilaya, G. Petriashvili, R. Barberi, R. Bartolino, G. Cipparrone, A. Mazzulla, L. Oriol, *Appl. Phys. Lett.* **2003**, *83*, 5353.
[119] A. Chanishvili, G. Chilaya, G. Petriashvili, R. Barberi, R. Bartolino, G. Cipparrone, A. Mazzulla, L. Oriol, *Adv. Mater.* **2004**, *16*, 791.
[120] T. H. Lin, Y. J. Chen, C. H. Wu, A. Y. G. Fuh, J. H. Liu, P. C. Yang, *Appl. Phys. Lett.* **2005**, *86*, 161120.
[121] L. Chen, Y. Li, J. Fan, H. K. Bisoyi, D. A. Weitz, Q. Li, *Adv. Opt. Mater.* **2014**, *2*, 845.
[122] Z. Zheng, B. W. Liu, L. Zhou, W. Wang, W. Hu, D. Shen, *J. Mater. Chem. C* **2015**, *3*, 2462.
[123] Z. Fan, A. O. Govorov, *Nano Lett.* **2010**, *10*, 2580.
[124] V. E. Bochenkov, D. S. Sutherland, *Opt. Express* **2018**, *26*, 27101.